

# Study on Molecular Assemblies Composed of Dual-stimuli Responsive Polymers and Applications for Chiral Separation Systems

多重刺激応答性高分子よりなる分子集合体の構築と、その光学分離システムへの応用に関する研究

2014

Meng Yu

## **Acknowledgements**

I would first like to acknowledge the financial support from the program of international program in Nagoya Institute of Technology funded by the Japanese government. With this program I can come to Japan for my further education and doing the research that I interested in. Thanks to the scholarship that provided by the MEXT, I can whole-heartedly devoted into my research and experienced the different life style with unique culture. These three years that I spend in Japan is delightful and memorable, all the experiences in Japan will play important part in my life.

My sincerely gratitude goes first and foremost for Professor Masahiro Higuchi, my supervisor, who always giving me advices and suggestions throughout my research. Only with the great help of Professor Higuchi, I can graduate on time. I also thank to Professor Higuchi for the careful revising and submitting of my paper and doctoral thesis. And I am very appreciated for the kindness help for my daily life in Japan.

Thanks to Professor Akinori Takasu, Professor Kenji Nagata for their instruction and support for my experiments. I also thank to Assistant Professor Daisuke Ishii, Doctor Tang Tang, Doctor Kazuki Murai and every students in the laboratory of Professor Masahiro Higuchi for their help in many respects.

I will thank to Professor Wantai Yang for reviewing the doctor thesis and giving some useful advices. Finally, I should show my great appreciate to my wife Haijing Liu and my parents for their support and trust for the past years. I am also thanks to my friends from heart for their encouraging.

# Content

<b>Chapter 1 Introduction.....</b>	<b>1</b>
<b>Chapter 2 Design and Synthesis of Amphiphilic Peptide.....</b>	<b>6</b>
2-1 Introduction .....	6
2-2 Design of Amphiphilic Peptide.....	6
2-2 Peptide synthesis.....	7
2-3 Characterization of peptide.....	8
2-4 Result and Discussion.....	9
2-5 Conclusion .....	14
<b>Chapter 3 pH and Thermo-induced Morphological Changes of the Amphiphilic Peptide Grafted Copolymer Assembly in Solution .....</b>	<b>17</b>
3-1 Introduction .....	17
3-2 Experimental Section.....	18
3-2-1 Preparation of Peptide Grafted Copolymer .....	18
3-2-2 Circular Dichroism (CD) Measurment .....	19
3-2-3 Transmittance Fourier Transform Infrared (TM-FTIR) Spectroscopy .....	20
3-2-4 Transmission Electron Microscopy (TEM) Observation.....	20
3-3 Results and Discussion .....	21
3-3-1 pH-induced conformational changes of peptide grafted copolymer.....	21
3-3-2 pH- and thermo- complex induced conformational changes of LKNIPAm ...	23
3-3-3 pH- and thermo-induced morphological changes of LKNIPAm in aqueous solution .....	26
3-4 Photo-initiated Peptide Grafted PNIPAm.....	28
3-4-1 Preparation of Peptide Grafted Copolymer .....	28
3-4-2 Characterization of Photo-initiated Copolymer .....	29
3-5 Conclusions .....	30

## **Chapter 4 pH- and Thermo-induced Specific Permeability of Chiral Amino Acids through the Peptide Grafted Poly(*N*-isopropylamide)**

### **Network Membrane.....34**

4-1 Introduction ..... 34

4-2 Experimental Section..... 35

4-2-1 Materials ..... 35

4-2-2 Preparation of polymer membrane ..... 36

4-2-3 Characterization of the peptide grafted membrane..... 36

4-2-4 FT-IR measurements ..... 37

4-2-5 Permeability measurements ..... 38

4-3 Result and Discussion..... 39

4-3-1 Degree of hydration and elongation of the membrane affected by external conditions ..... 39

4-3-2 pH-induced conformational transition of the peptides graft chain in the membrane ..... 40

4-3-3 Permselectivity of *L*- and *D*-phenylalanine induced by pH and thermal stimuli ..... 42

4-4 Effect of Crosslinking Degree on the Peptide-grafted Membrane ..... 44

4-4-1 effect of crosslinking degree for conformational changes of the peptide graft chains..... 44

4-4-2 Effect of crosslinking degree on the permeability changes of *L*- and *D*-Phe... 45

4-5 Conclusion ..... 47

## **Chapter 5 Controlled Release of Enantiomers in Peptide Grafted PNIPAm Gels.....51**

5-1 Introduction ..... 51

5-2 Experimental Section..... 52

5-2-1 Preparation of peptide grafted PNIPAm gels..... 52

5-2-2 Swelling study of PNIPAm gels ..... 53



5-2-3 FT-IR measurements .....	53
5-2-4 Release study of the gels .....	54
5-3 Results and discussion .....	54
5-3-1 degree of hydration of the swollen peptide grafted PNIPAm gels.....	54
5-3-2 pH-induced conformational transition of the peptides graft chain in the PNIPAm gel .....	55
5-3-3 Stimuli-induced controlled release of L- and D- phenylalanine .....	56
5-4 Conclusion .....	59
<b>Chapter 6 Conclusion .....</b>	<b>63</b>
<b>Publications .....</b>	<b>66</b>
<b>Conference .....</b>	<b>66</b>

# Chapter 1

## Introduction

Stimuli-responsive polymers are defined as polymers that undergo relatively large and abrupt, physical or chemical changes in response to small external changes in the environmental conditions. These polymer systems might recognize the stimuli's as signals, judge the magnitude of the signals, and then change their chain conformation in direct response<sup>1</sup>. There are many different stimuli to modulate the response of polymer systems. These stimuli could be classified as either physical or chemical stimuli. Chemical stimuli, such as pH, ionic strength and chemical agents, will change the interactions between polymer chains or between polymer chains and solvents at the molecular level. The physical stimuli, such as temperature, electric or magnetic fields, and mechanical stress, will affect the level of various energy sources and alter molecular interactions at critical onset points. These responses of polymer systems are very useful in bio-related applications such as drug delivery<sup>2-4</sup>, biotechnology<sup>3,5</sup>, chromatography<sup>6,7</sup>, nanotechnology<sup>8,9</sup> and a promising future for applications in the areas of biosensors and molecular separate membranes. Among these stimuli responsive polymers, temperature and pH responsive polymers have been the most intensively investigated in various laboratories and industries due to their relatively effective control in vivo as well as in vitro and their versatile application range.

Temperature is the most widely used stimulus in environmentally responsive polymer systems. The change of temperature is not only relatively easy to control, but also easily applicable both in vitro and in vivo. One of the unique properties of the temperature-responsive polymers is the presence of a critical solution temperature. Critical solution temperature is the temperature, at which the phase of polymer and solution is discontinuously changed. If the polymer solution has one phase below a specific temperature, which depends on the polymer concentration, and are phase-separated above this temperature, the polymer generally have a lower critical solution temperature (LCST). These polymers are usually composed of hydrophilic segment and suitable hydrophobic segment, and are mostly block copolymers. The

polymer solution having LCST shows the phase-separation upon heating due to the decrease of hydration of the hydrophilic segment and increase of the hydrophobic interaction among the hydrophobic segments. Up to date, poly(*N*-isopropylacrylamide) (PNIPAm) and its copolymers have been some of the most extensively studied LCST polymer. The reason for PNIPAm had so widely studied in all of polymer science due in most part to the readily accessible LCST of 32°C in water, just below physiological temperature (37°C). Moreover, the LCST of PNIPAm can be tuned by controlling the molecular weight or via incorporation of hydrophilic or hydrophobic groups<sup>10</sup>.

A pH-induced conformational change is common behavior in biopolymers. The pH-responsive polymers consist of ionizable pendants that can accept and donate protons in response to the environmental changes in pH. As the environmental pH changes, the degree of ionization in a polymer bearing weakly ionizable groups is dramatically altered at a specific pH that is called  $pK_a$ . This rapid change in net charge of pendant groups causes an alternation of the hydrodynamic volume of the polymer chains. The transition from collapsed state to expanded state is explained by the osmotic pressure exerted by mobile counterions neutralizing the network charges<sup>11</sup>. The polymers containing ionizable groups in their backbone form polyelectrolytes in the aqueous system. There are two types of pH-responsive polyelectrolytes; weak polyacids and weak polybases. The representative acidic pendant group of weak polyacids is the carboxylic group. Weak polyacids such as poly(acrylic acid) accept protons at low pH and release protons at neutral and high pH<sup>12</sup>. On the other hand, polybases like poly(4-vinylpyridine) is protonated at high pH and positively ionized at neutral and low pH<sup>13</sup>. Therefore, the proper selection between polyacids and polybases should be considered for the desired application.

Synthetic polypeptides, consisting of amino acids bearing ionizable pendant groups such as cysteine ( $pK_a=8.4$ ), aspartic acid ( $pK_a=3.9$ ), glutamic acid ( $pK_a=4.1$ ), histidine ( $pK_a=6.0$ ), lysine ( $pK_a=10.5$ ), or arginine ( $pK_a=12.5$ )<sup>14</sup>, might undergo a pH responsive conformational transition at around their  $pK_a$ . For example, poly(glutamic acid) has carboxylic groups in its side chains and undergoes a sharp phase transition by helix to coil conformational change at a pH a little bit higher than its  $pK_a$ .

Some systems have been developed to combine two or more stimuli-responsive mechanisms into one polymer system. Some workers have reported that two or more signals could be simultaneously applied in order to induce response in so-called dual responsive polymer systems. The hierarchical structures of the stimuli-responsive block copolymers formed via self-assemblies are generally dependent on the structure and property of each segment, composition, and chain length, in addition to external stimuli such as pH, ionic strength, and temperature. For the precise manipulation of the dual-responsive properties and stimuli-induced self-assembling behaviors, such as normal and reversible micelle formation, it is important to create block polymers composed of two stimuli-sensitive segments, each of which should possess narrow chain length distributions with controlled molar mass and composition. The design and synthesis of novel block copolymers derived from peptides are attracting significant attention because of their assembled structures through intra- and interchain associations via noncovalent bonds and their potential applications as biodegradable and biomedical polymers<sup>15-17</sup>. In peptide based block copolymers, the nature of amino acids and the chirality and amphiphilicity encoded in their primary structures play crucial roles in determining their ordered structures and various functions.

In our thesis, we based on the thermal-sensitive poly(N-isopropylacrylamide) design a dual-responsive polymer. We introduce the amphiphilic graft chain peptide, which was sensitive to the pH condition, to the PNIPAm chain. The novel copolymer was sensitive to both temperature and pH, we also investigated the application of this copolymer.

## Reference

1. Eun Seok Gil & Samuel M. Hudson, Stimuli-responsive polymers and their bioconjugates, *Progress in Polymer Science*. **29**, 1173-1222 (2004).
2. Piyush Gupta, Kavita Vermani & Sanjay Garg, Hydrogels: from controlled release to

- pH-responsive drug delivery, *Drug Discovery Today*. **7**, 569-579 (2002).
3. Byeongmoon Jeong&Anna Gutowska, Lessons from nature: stimuli-responsive polymers and their biomedical applications, *Trends in Biotechnology*. **20**, 305-311 (2002).
  4. Yong Qiu&Kinam Park, Environment-sensitive hydrogels for drug delivery, *Advanced Drug Delivery Reviews*. **53**, 321-339 (2001).
  5. Igor Y. Galaev&Bo Mattiasson, 'Smart' polymers and what they could do in biotechnology and medicine, *Trends in Biotechnology*. **17**, 335-340 (1999).
  6. Akihiko Kikuchi&Teruo Okano, Intelligent thermoresponsive polymeric stationary phases for aqueous chromatography of biological compounds, *Progress in Polymer Science*. **27**, 1165-1193 (2002).
  7. Jun Kobayashi,Akihiko Kikuchi,Kiyotaka Sakai&Teruo Okano, Aqueous chromatography utilizing hydrophobicity-modified anionic temperature-responsive hydrogel for stationary phases, *Journal of Chromatography A*. **958**, 109-119 (2002).
  8. Hiromi Hamamoto,Yachiyo Suzuki,Yoichi M. A. Yamada,Hidetsugu Tabata,Hideyo Takahashi&Shiro Ikegami, A Recyclable Catalytic System Based on a Temperature-Responsive Catalyst, *Angewandte Chemie*. **117**, 4612-4614 (2005).
  9. Craig E. Banks,Alison Crossley,Christopher Salter,Shelley J. Wilkins&Richard G. Compton, Carbon Nanotubes Contain Metal Impurities Which Are Responsible for the "Electrocatalysis" Seen at Some Nanotube-Modified Electrodes, *Angewandte Chemie International Edition*. **45**, 2533-2537 (2006).
  10. Piotr Kujawa,Florence Segui,Sherry Shaban,Charbel Diab,Yukinori Okada,Fumihiko Tanaka&Françoise M. Winnik, Impact of End-Group Association and Main-Chain Hydration on the Thermosensitive Properties of Hydrophobically Modified Telechelic Poly(N-isopropylacrylamides) in Water, *Macromolecules*. **39**, 341-348 (2005).
  11. S. R. Tonge&B. J. Tighe, Responsive hydrophobically associating polymers: a review of structure and properties, *Advanced Drug Delivery Reviews*. **53**, 109-122 (2001).
  12. Olga E. Philippova,Dominique Hourdet,Roland Audebert&Alexei R. Khokhlov, pH-Responsive Gels of Hydrophobically Modified Poly(acrylic acid), *Macromolecules*. **30**, 8278-8285 (1997).
  13. V. T. Pinkrah,M. J. Snowden,J. C. Mitchell,J. Seidel,B. Z. Chowdhry&G. R. Fern,

Physicochemical Properties of Poly(N-isopropylacrylamide-co-4-vinylpyridine) Cationic Polyelectrolyte Colloidal Microgels, *Langmuir*. **19**, 585-590 (2003).

14. Moran LA Horton HR, Ochs RS, Rawn JD, Scrimgeour KG, Principles of biochemistry; Prentice Hall: Upper Saddle River, New Jersey, 2002.

15. Matthias Meyer & Helmut Schlaad, Poly (2-isopropyl-2-oxazoline)-poly (L-glutamate) block copolymers through ammonium-mediated NCA polymerization, *Macromolecules*. **39**, 3967-3970 (2006).

16. Kemal Arda Günay, Patrick Theato & Harm-Anton Klok, Standing on the shoulders of Hermann Staudinger: Post-polymerization modification from past to present, *Journal of Polymer Science Part A: Polymer Chemistry*. **51**, 1-28 (2013).

17. Harm-Anton Klok, Josef F Langenwaller & Sébastien Lecommandoux, Self-assembly of peptide-based diblock oligomers, *Macromolecules*. **33**, 7819-7826 (2000).

## Chapter 2

### Design and Synthesis of Amphiphilic Peptide

#### 2-1 Introduction

In nature, the amino acids are combined to give proteins with hundreds or even thousands of amino acids in each one. Small assemblies of amino acids are known as peptides. With increased research in the areas of molecular and biological chemistry, the need for an efficient and simple method of peptide synthesis became apparent. In 1963 Merrifield<sup>1</sup> developed the method which called solid phase peptide synthesis (SPPS) provided the revolution for this demand. This technique utilizes an insoluble solid support of polystyrene copolymer beads as an anchor for the synthetic peptide chain. The terminal amino acid is bound to the resin support and the protected amino acids are added individually in a sequential series of manual or automated steps. The completed peptide is then cleaved from the resin. Principally, peptide synthesis relies on the appropriate combination of protecting groups and an efficient method for the activation of the carboxyl group prior to reaction with the amino group for growth of the peptide chain in the C-to-N direction. Thus, a general solid-phase peptide synthesis scheme includes a *N*-amino protecting group (temporary protecting group), side-chain protecting groups (permanent protecting groups) and a linker, a specialized protecting group that attaches the peptide to the support.

Design and synthesis process of the peptide used in this study are described in this chapter. To prepare the dual-responsive polymer, few kinds of amphiphilic peptide were synthesized. These peptides could form well-defined secondary structure, and we investigated the conformational changes induced by pH conditions. In this study, peptides were synthesized by the solid-phase method using standard Fmoc-strategy on CLEAR-Acid resin.

#### 2-2 Design of Amphiphilic Peptide

Based on the purpose of our study, we need a kind of amphiphilic peptide which could responsive to external pH changes. Considering the previous work<sup>2-5</sup> of our group, we designed three kinds of peptides. The sequences of peptide (LK)<sub>8</sub>-vinyl, (LKLQ)<sub>4</sub>-vinyl and (LELK)<sub>4</sub>-vinyl were shown in Fig. 2-1.

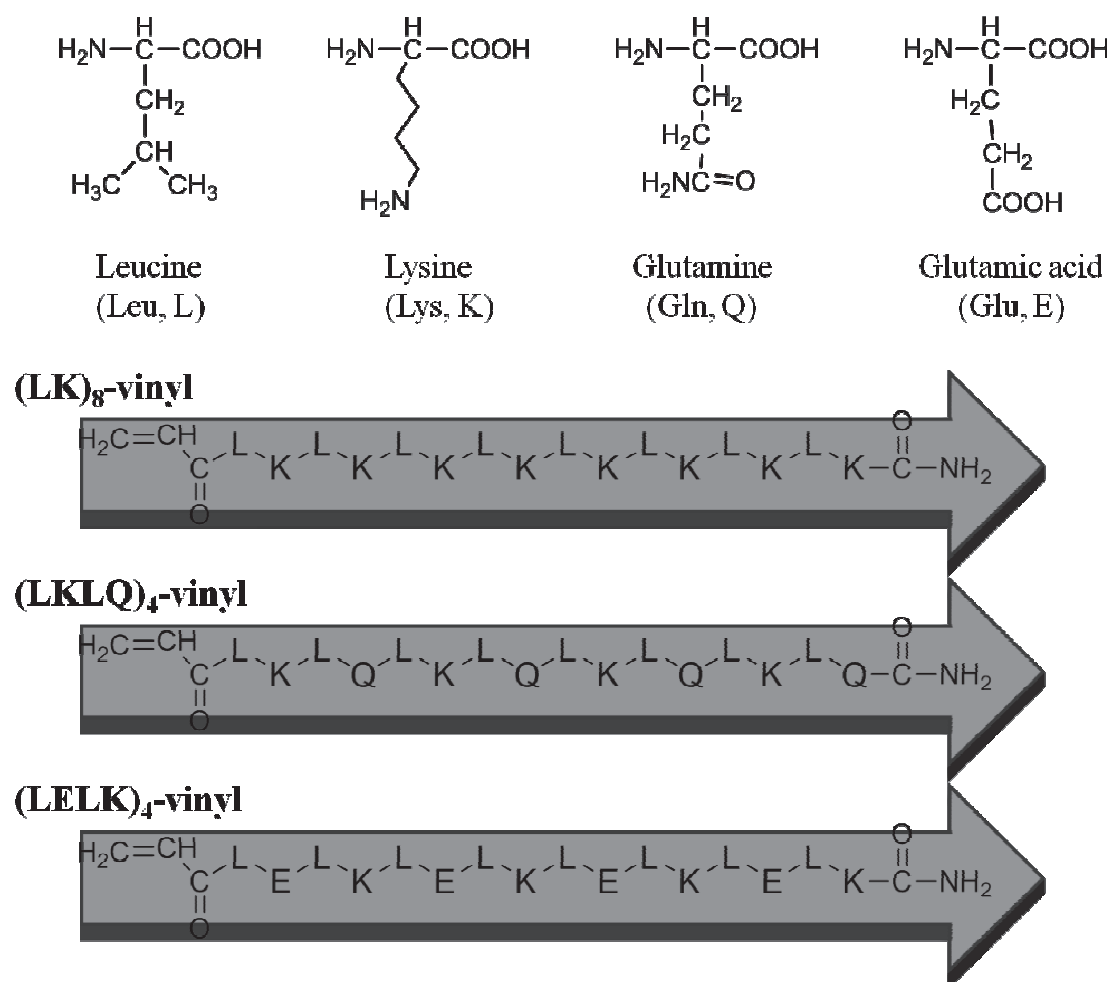


Fig. 2-1. Chemical structures of amino acids and sequence of synthesized peptides.

## 2-2 Peptide synthesis

The peptides were synthesized according to the conventional solid-phase method<sup>6</sup>. Take the peptide (LK)<sub>8</sub>-vinyl as example, the peptide chain was synthesized on a CLEAR-acid resin (cross-linked ethoxylate acrylated resin, Peptide Institute), using Fmoc-amino acid derivatives (3 equiv), 1-hydroxy-7-azabenzotriazole (HOAt) (3 equiv), and 1,3-diisopropylcarbodiimide (DIPCDI) (3 equiv) in



*N,N*-dimethylformamide (DMF) for coupling and using piperidine (25 vol%) / DMF to remove the Fmoc. The acrylic acid was then attached to the *N*-terminal of the peptide on the resin using the same protocol described above. After the coupling

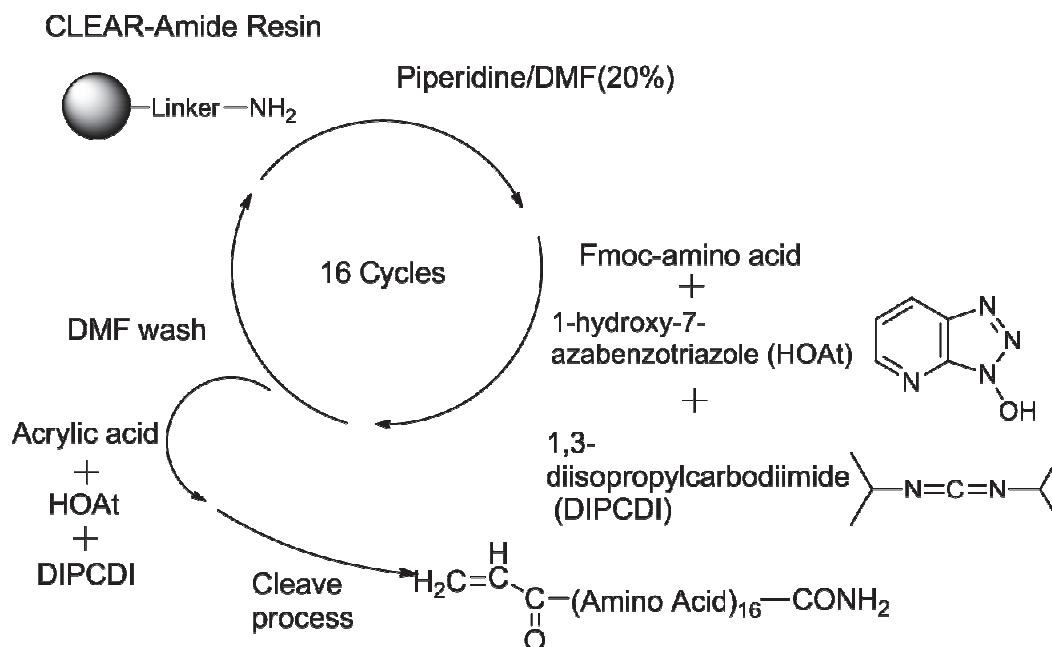


Fig. 2-2. Scheme of solid phase peptide synthesis

reactions, to cleave the (Leu-Lys)<sub>8</sub>-vinyl from the resin and to remove the side-chain protecting groups, the peptide-resin was treated with cooled aqueous solution containing 95 vol% trifluoroacetic acid (TFA). After the reaction, the mixture was filtered to separate the peptide solution from the resin support. The TFA solution of the peptide was concentrated to a volume of approximately 1-2 mL, and then 100 mL of cooled ether was added to precipitate the peptide. The synthesis process was shown in Fig. 2-2.

### 2-3 Characterization of peptide

Identification of synthesized peptides were performed by Matrix Assisted Laser Desorption Ionization-Time of Flight Mass Spectroscopy (MALDI-TOF-MS) (JMS-S3000, JEOL).

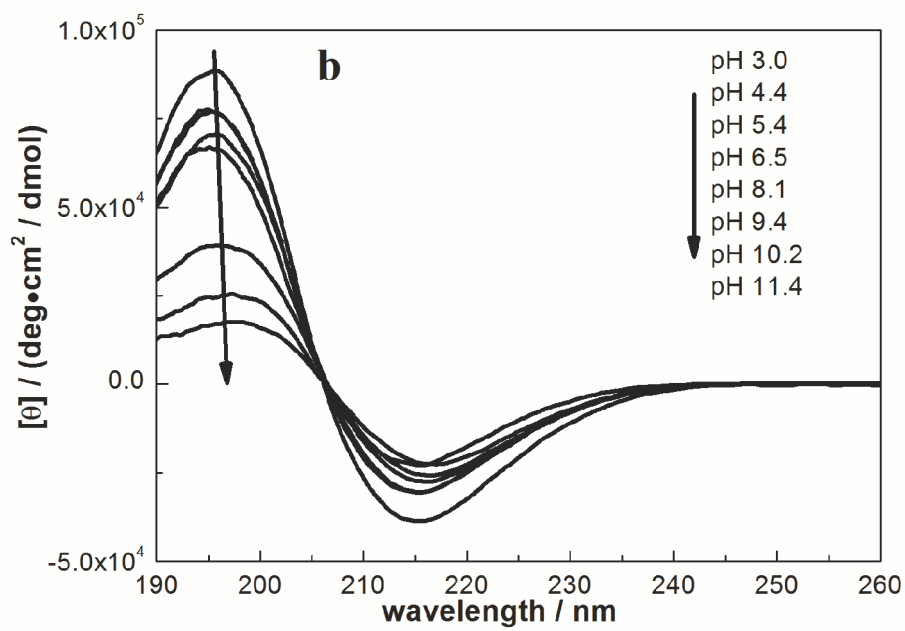
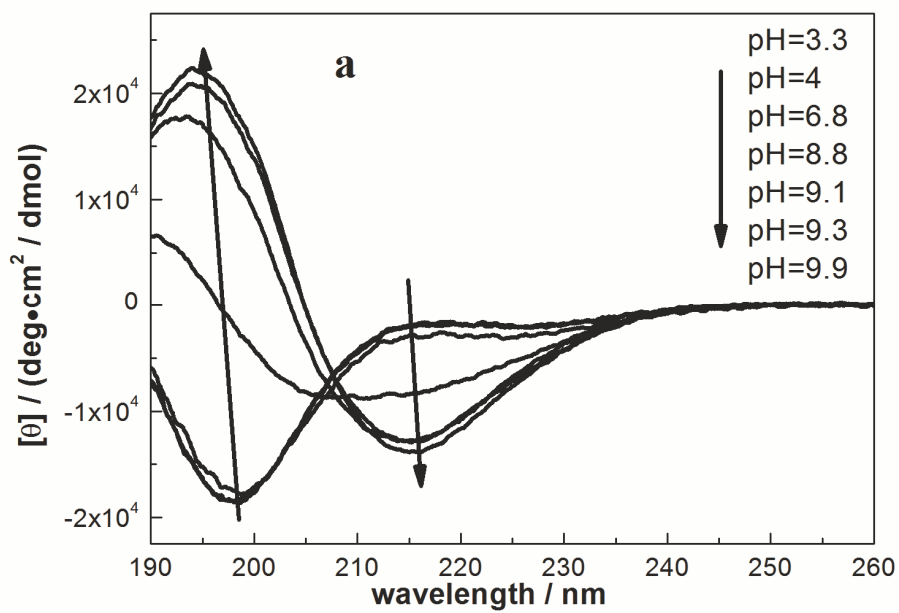
The pH-induced conformational changes of peptides in aqueous solution were investigated by means of circular dichroism (CD). CD spectra were recorded on a

J-820 spectrophotometer (JASCO) under a nitrogen atmosphere. Experiments were performed in a quartz cell with 0.1 cm path length from 190 to 250 nm at ambient temperature. The pH of the solution was adjusted with 0.1 M HCl or 0.1 M NaOH.

## 2-4 Result and Discussion

Sequential alternating amphiphilic peptides composed of hydrophobic and hydrophilic amino acids have been shown to take a  $\beta$ -sheet structure and form fibrous assemblies under specific conditions, such as a certain pH and/or solvent composition<sup>7,8</sup>. The pH-induced conformational changes of peptides were characterized by CD. The concentration of peptide was fixed at 0.8 mM. Fig. 2-3 shows the pH-induced CD spectral changes of peptides in aqueous solution.

It is clearly showed in Fig. 2-3 that these three peptides show different conformation transition behavior as pH increased from acidic to basic. At acidic condition, the CD spectrum of peptide (LK)<sub>8</sub>-vinyl show a negative peak at 198 nm indicated a random coil conformation. Under basic conditions, the CD spectra of (Leu-Lys)<sub>8</sub>-vinyl changed to a typical  $\beta$ -sheet pattern, which shows a negative maximum at 215 nm. This could be explained that at acidic condition, the amino groups of lysine were protonated and the electro static repulsion disturbed the formation of intermolecular hydrogen bond led to the random coil structure. However,



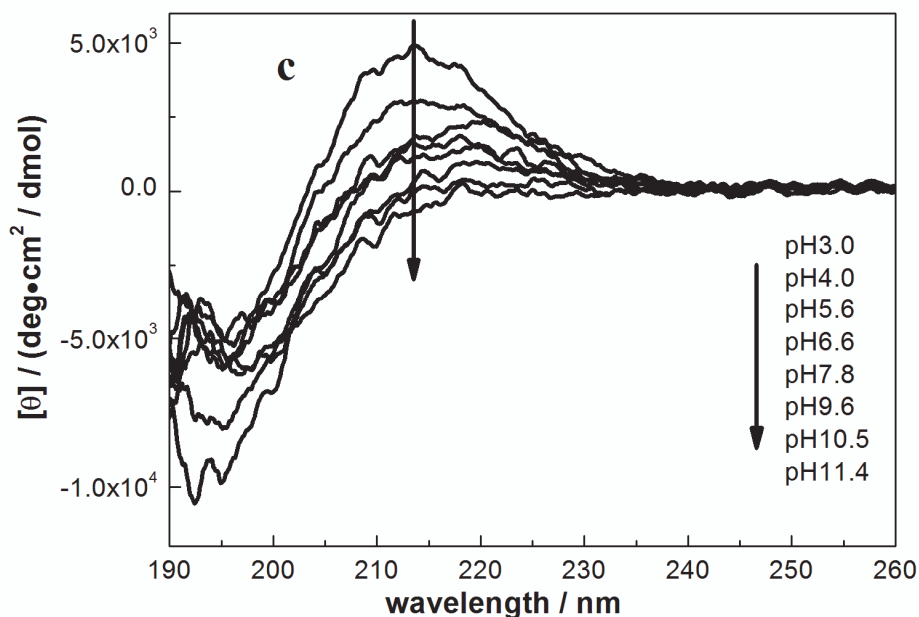


Fig. 2-3. CD spectrum of 0.8 mM synthesized peptide a); (LK)<sub>8</sub>-vinyl, b); (LKLQ)<sub>4</sub>-vinyl, c); (LELK)<sub>4</sub>-vinyl in aqueous solution at ambient temperature. The curves under various pH conditions were arranged according to the arrow direction.

at basic condition the amino groups of the Lys moieties were deprotonated and  $\beta$ -sheet structure formed because of intermolecular hydrogen bond.

For the peptide (LKLQ)<sub>4</sub>-vinyl, the CD spectrum always show a negative peak at 215 nm and a positive peak at 196 nm, which means this peptide formed  $\beta$ -sheet pattern under both acidic and basic conditions. However, the negative value of  $[\theta]_{215}$  was decrease with pH increasing. This implies that the  $\beta$ -sheet conformation was decreased under the basic condition. The distinction of conformational behavior under the acidic condition between the (LK)<sub>8</sub>-vinyl and (LKLQ)<sub>4</sub>-vinyl could be explained as follows. The electro static repulsion among the protonated amino groups of the Lys moieties in the case of (LKLQ)<sub>4</sub>-vinyl was lower than that of (LK)<sub>8</sub>-vinyl. So that the (LKLQ)<sub>4</sub>-vinyl formed  $\beta$ -sheet structure under the acidic condition. Furthermore, the amide side chains of the glutamine residues have a strong tendency to form hydrogen bond with each other<sup>9-11</sup>. The hydrogen bond among the amide side chains of the deprotonated (LKLQ)<sub>4</sub>-vinyl led to the formation of disordered assembly of the

(LKLQ)<sub>4</sub>-vinyl. As a result the  $\beta$ -sheet structure ratio was decreased as pH increased, especially when pH was higher than 7.0 the  $\beta$ -sheet structure has an obviously decrease (Fig. 2-3b). The (LELK)<sub>4</sub>-vinyl took a random coil conformation under the both acidic and basic conditions. The CD spectra in Fig. 2-3c of (LELK)<sub>4</sub>-vinyl showed typical CD spectra assumed random coil conformation with a negative peak around 197 nm. We think the complementary ionic bridge is still the reason for this phenomenon. The ionic bridge was formed between amino group of lysine residue and carboxyl group of glutamic acid residue both intermolecular and intramolecular. The ionic bridge resulted to the formation of disordered aggregate of the (LELK)<sub>4</sub>-vinyl in aqueous solution. This suppose was supported by the high tension voltage (HT) data. The high value of HT means high turbidity which indicated the formation of the aggregate. The CD spectrum only slightly changed as pH increased from 3.0 to 11.4. Similar examples were seen in oligopeptides (i + 4) E,K and (i + 4) K,E where a change of pH had little effect on their stability<sup>12</sup>.

Considering the purpose of our study that we need a pH-responsive amphiphilic peptide, so we choose peptide (LK)<sub>8</sub>-vinyl as the pH-sensitive part of the grafted polymer. So we further investigated the pH-induced conformational transition of (LK)<sub>8</sub>-vinyl. Fig 2-4 was the CD spectra of (LK)<sub>8</sub>-vinyl for the reversibility pH changes, when the pH of the solution was increased (Fig 2-4a) and decreased (Fig 2-4b). From the spectra we could found out that the pH-induced conformational changes were reversible, when the pH increased from acidic to basic condition the peptide transformed from random coil to  $\beta$ -sheet conformation; meanwhile, as pH decreased from basic to acidic the secondary structure of peptide revised from  $\beta$ -sheet

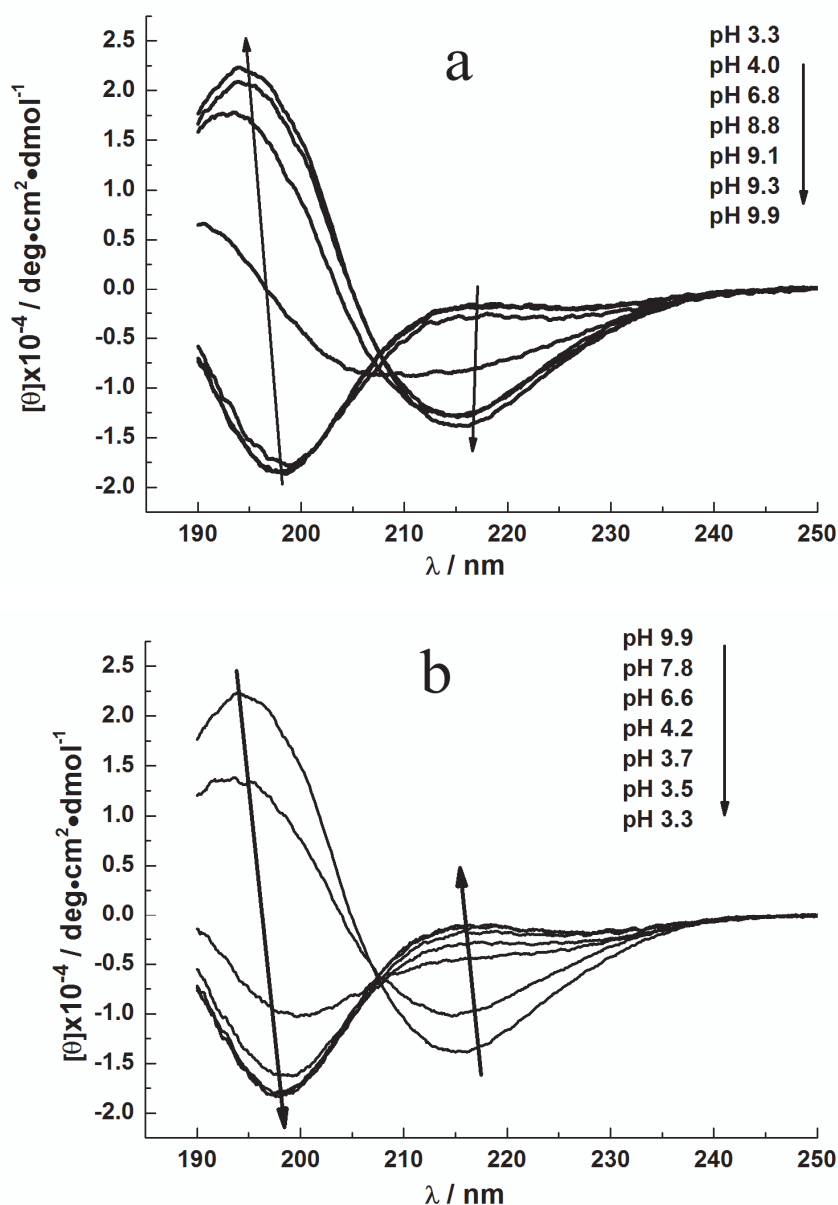
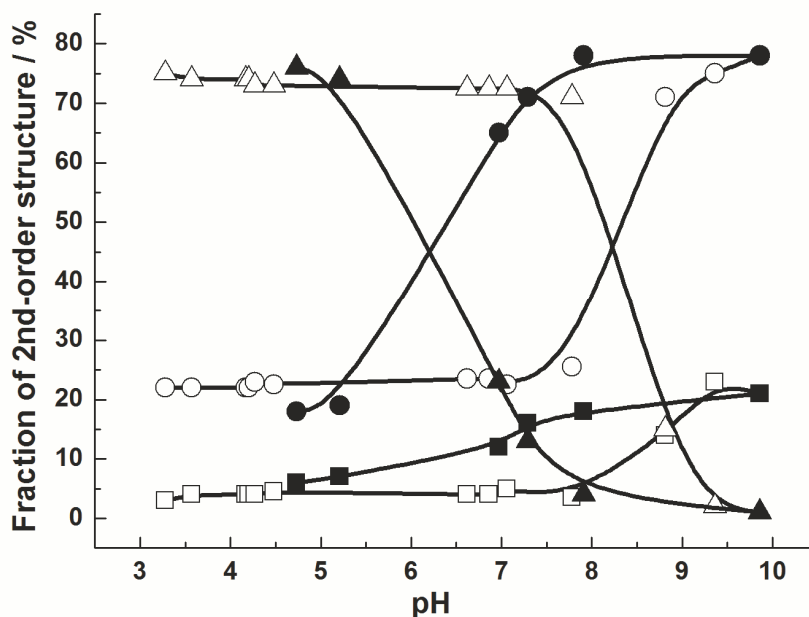


Fig. 2-4. CD spectrum of peptide (LK)<sub>8</sub>-vinyl as pH increased (a) and decreased (b)

to random coil conformation. The fraction of second-order structure was calculated using a quantitative curve-fitting analysis of the CD spectrum according to a linear combination of typical CD spectra for dispersed  $\alpha$ -helical,  $\beta$ -sheet, and random coil conformations<sup>13</sup>. The percentages of each structure under various pH conditions were marked in Fig 2-5. The reversibility of the conformational transition could be obviously observed. However, a considerable hysteresis was observed in the



**Fig. 2-5.** pH dependence of the fraction of second-order structure. □, ■:  $\alpha$ -helix, ○, ●:  $\beta$ -sheet, and △, ▲: random coil conformation of (Leu-Lys)<sub>8</sub>-vinyl estimated from the CD-curve fitting method. The open and closed symbols denote the fraction of the second-order structure when the pH of the solution was increased and decreased, respectively.

pH-induced transition.

## 2-5 Conclusion

In this chapter, we synthesized three kinds of 16-residue amphipilic peptides, (LK)<sub>8</sub>-vinyl, (LKLQ)<sub>4</sub>-vinyl, (LELK)<sub>4</sub>-vinyl. The secondary structure of each peptide under various pH conditions was characterized by the Circular Dichroism spectrum. From the investigation we found that only (LK)<sub>8</sub>-vinyl has the responsibility to pH conditions, which changed from random coil conformation under acidic condition to  $\beta$ -sheet structure under basic condition. Moreover, the pH-induced conformational change of this peptide was also reversible. According to the purpose of our study, we chose the peptide (LK)<sub>8</sub>-vinyl as the pH-sensitive part of the dual-responsive grafted polymer.

## Reference

1. R. B. Merrifield, Solid Phase Peptide Synthesis. I. The Synthesis of a Tetrapeptide, *Journal of the American Chemical Society*. **85**, 2149-2154 (1963).
2. Tomoyuki Koga, Kazuhiro Taguchi, Takatoshi Kinoshita & Masahiro Higuchi, pH-Regulated formation of amyloid-like  $\beta$ -sheet assemblies from polyglutamate grafted polyallylamine, *Chem. Commun.*, 242-243 (2002).
3. Tomoyuki Koga, Kazuhiro Taguchi, Yoshiaki Kobuke, Takatoshi Kinoshita & Masahiro Higuchi, Structural Regulation of a Peptide-Conjugated Graft Copolymer: A Simple Model for Amyloid Formation, *Chemistry-a European Journal*. **9**, 1146-1156 (2003).
4. Masahiro Higuchi, Takateru Inoue, Hidenori Miyoshi & Masami Kawaguchi, pH-induced reversible conformational and morphological regulation of polyleucine grafted polyallylamine assembly in solution, *Langmuir*. **21**, 11462-11467 (2005).
5. Masahiro Higuchi & Takatoshi Kinoshita, Specific Permeability of Chiral Amino Acids through Functional Molecular Membranes Composed of an Amphiphilic Graft Peptide, *ChemPhysChem*. **9**, 1110-1113 (2008).
6. Louis A Carpino & Grace Y Han, 9-Fluorenylmethoxycarbonyl amino-protecting group, *The Journal of Organic Chemistry*. **37**, 3404-3409 (1972).
7. Dong-Pyo Hong, Masaru Hoshino, Ryoichi Kuboi & Yuji Goto, Clustering of fluorine-substituted alcohols as a factor responsible for their marked effects on proteins and peptides, *Journal of the American Chemical Society*. **121**, 8427-8433 (1999).
8. Tomoyuki Koga, Miho Matsuoka & Nobuyuki Higashi, Structural Control of Self-Assembled Nanofibers by Artificial  $\beta$ -Sheet Peptides Composed of d- or l-Isomer, *Journal of the American Chemical Society*. **127**, 17596-17597 (2005).
9. David A. Dixon, Kerwin D. Dobbs & James J. Valentini, Amide-Water and Amide-Amide Hydrogen Bond Strengths, *The Journal of Physical Chemistry*. **98**, 13435-13439 (1994).
10. Irving M. Klotz & Sutton B. Farnham, Stability of an amide-hydrogen bond in an apolar environment, *Biochemistry*. **7**, 3879-3882 (1968).



11. A. T. Hagler&L. Leiserowitz, The amide hydrogen bond and the anomalous packing of adipamide, *Journal of the American Chemical Society*. **100**, 5879-5887 (1978).
12. S. Marqusee&R. L. Baldwin, Helix stabilization by Glu-...Lys+ salt bridges in short peptides of de novo design, *Proceedings of the National Academy of Sciences of the United States of America*. **84**, 8898-8902 (1987).
13. Norma J. Greenfield&Gerald D. Fasman, Computed circular dichroism spectra for the evaluation of protein conformation, *Biochemistry*. **8**, 4108-4116 (1969).

# Chapter 3

## pH and Thermo-induced Morphological Changes of the Amphiphilic Peptide Grafted Copolymer Assembly in Solution

### 3-1 Introduction

In the last decade, various fields have focused considerable attention on stimuli-responsive polymers<sup>1</sup>. These polymers can be used in drug delivery, tissue engineering, biosensing, and separation processes due to their sensitivity to environmental conditions<sup>2-4</sup>. There are many possible stimuli, such as temperature, pH, light, and electric fields; most intensive investigations have focused on temperature- and pH-responsive polymers for biomedical applications<sup>5,6</sup>. To date, most dual thermo- and pH-sensitive polymers are prepared by incorporating pH-responsive ionic components such as carboxyl and amino groups into thermo-sensitive polymer. Thermo-sensitive polymers exhibit a lower critical solution temperature (LCST) in aqueous solution, below which the polymers are water-soluble and above which they become insoluble. Poly(*N*-isopropylacrylamide) (PNIPAm) and its copolymers are the most extensively studied LCST-type thermo-sensitive polymers. Polymers exhibiting LCST properties have potential applications for “intelligent” or “smart” materials. The thermo-responsive nature of these polymers has led to applications in drug delivery<sup>7</sup>, bioengineering<sup>8</sup>, and nanotechnology<sup>9</sup> and suggests a promising future for applications in the areas of biosensors and membranes.

Helices and  $\beta$ -sheets are the major secondary structural motifs organizing the three-dimensional geometry of proteins. The conformational and morphological changes of proteins and peptides induced by chemical and/or physical stimuli have attracted attention not only because of the functional regulation owing to their characteristic structure<sup>10</sup> but also because of their association with neurodegenerative diseases<sup>11</sup> such as Alzheimer’s and Creutzfeldt-Jacob’s. In previous studies<sup>12-14</sup>, we

reported that a simple amphiphilic copolymer, hydrophilic peptide-grafted polyallylamine, formed amyloid-like fibrils in aqueous solution under acidic conditions. The pH-induced reversible conformational transition was also observed<sup>15</sup>. Studies of the structural regulation for peptides forming a  $\beta$ -sheet may be important not only for understanding the pathogenesis and therapeutics of certain diseases but also for providing useful information for the development of nanobiomaterials with a wide range of applications, such as uses in nanodevices.

Peptide-conjugated PNIPAm systems have been widely studied<sup>16,17</sup>. Mezzenga<sup>18</sup> used poly(*N*-isopropylamide) conjugated with peptide to form biocompatible hydrogels, but these polymers were only responsive to single stimuli. In this paper, we describe the pH- and thermo-induced conformational and morphological changes of (leucine-lysine)<sub>8</sub>-grafted poly(*N*-isopropylacrylamide) in aqueous solution. In combining the pH-sensitive (Leu-Lys)<sub>8</sub> with the temperature-responsive PNIPAm, we demonstrated the creation of a multi-stimuli responsive polymer system. Under acidic conditions, the amino groups of the Lys moieties of the (Leu-Lys)<sub>8</sub> graft chains were protonated, and the electrostatic repulsion disturbed the formation of  $\beta$ -sheet structure. However, under basic conditions, the deprotonated (Leu-Lys)<sub>8</sub> graft chains could form  $\beta$ -sheet via inter-molecular hydrogen bonding. However, below the coil-to-globule transition temperature of the main chain, the inter-molecular hydrogen bonding among the (Leu-Lys)<sub>8</sub> graft chains was disturbed owing to the coil conformation. The (Leu-Lys)<sub>8</sub> graft chain took a stable  $\beta$ -sheet structure only under basic conditions and above the transition temperature. The  $\beta$ -sheet conformation induced the formation of large aggregates of the peptide-grafted copolymers. This multi-stimuli responsive polymer system could be useful for various applications, such as drug delivery and membrane separation.

## **3-2 Experimental Section**

### **3-2-1 Preparation of Peptide Grafted Copolymer**

The sequence (Leu-Lys)<sub>8</sub>-vinyl was chosen as a pH-dependent,  $\beta$ -sheet forming

element. The processes of peptide synthesis and pH-induced conformational transitions of peptides have been reported in Chapter 2.

The peptide was identified by MALDI-TOF mass spectroscopy (JMS-S3000, JEOL). The observed  $m/z$  of the peptide was 2023.9. This value was in fair agreement with the calculated value of 2024.7  $[M+Na]^+$ .

We chose PNIPAm as the thermo-responsive hydrophilic main chain of the grafted copolymer. The pH- and thermo-responsive graft copolymer, (Leu-Lys)<sub>8</sub>-grafted poly(*N*-isopropylacrylamide) (LKNIPAm), was prepared as followed. (Leu-Lys)<sub>8</sub>-vinyl (20 mg) and NIPAm (4.52 mg) were dissolved in aqueous solution. To remove the oxygen from the reaction mixture, three freeze-pump-thaw cycles were performed. The copolymerization of the (Leu-Lys)<sub>8</sub>-vinyl and NIPAm was initiated by AIBN in a conventional radical polymerization method. The AIBN (0.2 mg) was added to the reaction mixture, which was then stirred for 48 h at 70 °C. The reaction mixture was then precipitated into excess ether. The precipitate was dissolved in water, and the aqueous solution was dialyzed against water using a molecular porous membrane tube (BioDesign Inc. of New York, MWCO 3500). After the dialysis, the solution was lyophilized to obtain LKNIPAm. The graft peptide content of 12 mol% in LKNIPAm was estimated by means of <sup>1</sup>H-NMR spectroscopy in deuterated TFA, on the basis of the area ratio of the signal of -NH-CH-CO- ( $\delta=4.1$  ppm) of the peptide graft chain to that of -CH<sub>3</sub> ( $\delta=1.3$  ppm) of the methyl groups of the NIPAm and Leu side chains. The molecular weight of the obtained LKNIPAm was estimated by size exclusion chromatography (SEC), calibrated with polystyrene standards using a pump system of Tosoh DP8020 with a TSK-GEL  $\alpha$ -3000 column [eluent; DMF, flow rate; 0.5 mL/min, temperature; 40 °C]. The number average molecular weight of LKNIPAm was  $1.3 \times 10^4$  ( $M_w/M_n$  was 2.7).

### 3-2-2 Circular Dichroism (CD) Measurement

The pH-induced conformational changes of the peptide graft chain of the LKNIPAm in aqueous solution were investigated by means of circular dichroism (CD). CD spectra were recorded on a J-820 spectrophotometer (JASCO) under a

nitrogen atmosphere. Experiments were performed in a quartz cell with 0.1 cm path length from 190 to 250 nm at ambient temperature. The pH of the solution was adjusted with 0.1 M HCl or 0.1 M NaOH.

The thermo-induced turbidity changes of the LKNIPAm aqueous solution were investigated by means of their transmittance changes. The transmittance at 450 nm of the LKNIPAm aqueous solutions was measured with the J-820 spectrophotometer equipped with a temperature control accessory (PTC-423L, JASCO). The transmittance values at 450 nm were obtained by the conversion of the high tension voltage at 450 nm.

### **3-2-3 Transmittance Fourier Transform Infrared (TM-FTIR) Spectroscopy**

The thermo-induced changes in the secondary structure of the peptide graft chain in LKNIPAm were estimated by Transmittance Fourier transform infrared (TM-FTIR) spectroscopy. The TM-FTIR spectra were measured with a Perkin-Elmer Spectra 2000 (resolution: 4 cm<sup>-1</sup>, number of scan: 32). The LKNIPAm aqueous solutions at various pH and temperature were quickly frozen in liquid nitrogen, and then the frozen samples were lyophilized to obtain LKNIPAm powder. The pellets for TM-FTIR measurements were prepared by mixing the LKNIPAm powder with KBr. The weight fraction of the LKNIPAm was fixed at 1 wt%.

### **3-2-4 Transmission Electron Microscopy (TEM) Observation**

The morphology of LKNIPAm in aqueous solution at various pH and temperature was directly observed by transmission electron microscopy using a freeze-fracture etching replica technique.<sup>21,22</sup> An aliquot of the LKNIPAm solution at the designated pH and temperature was placed on a thin gold plate, and this sample was rapidly plunged into liquid nitrogen (EM-19510SNPD, JEOL). The sample was stored in liquid nitrogen until it fractured. Freeze-fracturing was carried out with a freeze-etching system (JFD-II, JEOL) at -170 °C and 3.4×10<sup>-5</sup> Pa, and then freeze-etching was performed at -120 °C and 3.5×10<sup>-5</sup> Pa for 15 min. To prepare the replica, platinum-carbon and pure carbon were evaporated at angles of 60° and 90°,

respectively, to the specimen surface. Electron microscopy was carried out using a JEOL z2500 electron microscope operating at 200 kV.

### 3-3 Results and Discussion

#### 3-3-1 pH-induced conformational changes of peptide grafted copolymer

We compared the pH-induced conformational transition of the peptide graft chain in the LKNIPAm with that of the free peptide, (Leu-Lys)<sub>8</sub>-vinyl. Fig. 3-1 shows the pH-induced CD spectral changes of LKNIPAm in aqueous solution. The CD measurements, as the pH of the solution were increased (Fig. 3-1a) and

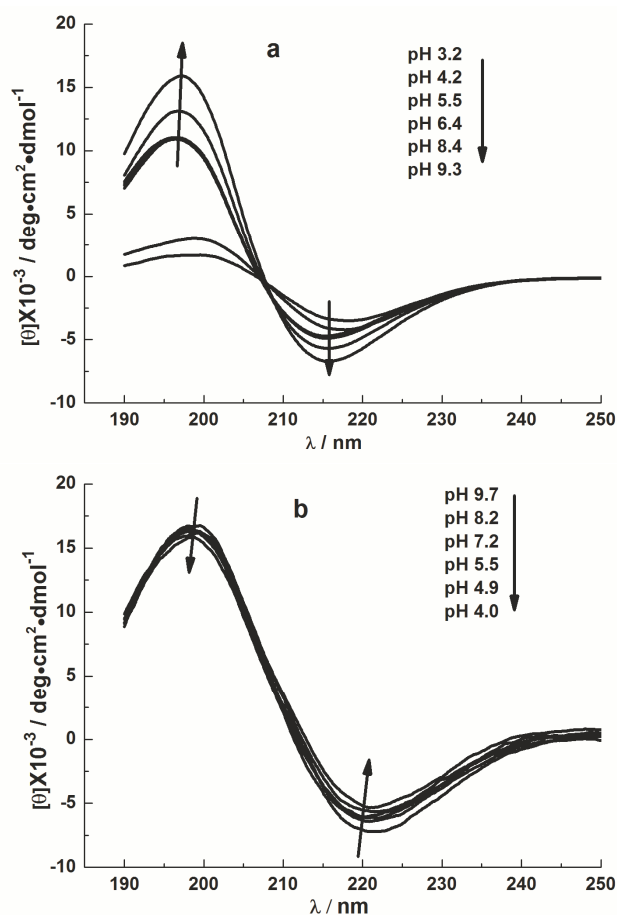


**Fig. 3-1.** pH-induced CD spectral changes of LKNIPAm in aqueous solution. The CD measurements at (a) increasing pH and (b) decreasing pH were carried out immediately after adjusting the pH of the sample solution.

decreased (Fig. 3-1b), were carried out immediately after the adjustment of the pH of the solution at ambient temperature. The concentration of the peptide graft chain was fixed at 0.03 mM. All the CD spectra of LKNIPAm showed a negative maximum at

approximately 218 nm, which indicates the existence of a  $\beta$ -sheet structure. As the graft peptide was fixed on the PNIPAm main chain, the local concentration of the graft peptide around the PNIPAm main chain was increased in comparison with the same concentration of the free peptide (Leu-Lys)<sub>8</sub>-vinyl. At equal concentrations of peptide (0.03 mM),  $[\theta]_{218\text{nm}}$  of LKNIPAm was larger than that of the free peptide, (Leu-Lys)<sub>8</sub>-vinyl. (Fig. 3-2), indicating that the (Leu-Lys)<sub>8</sub> graft chain of LKNIPAm could more easily adopt a  $\beta$ -sheet structure compared to the free peptide (Leu-Lys)<sub>8</sub>-vinyl, owing to the increased local concentration. In other words,

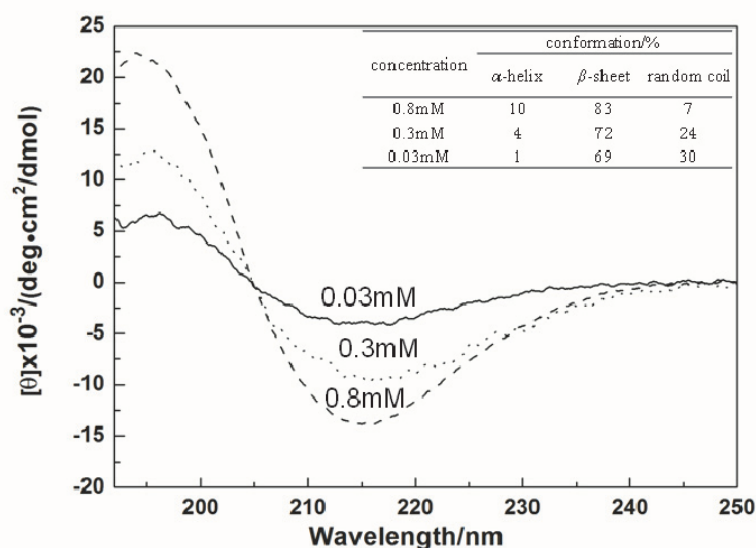


**Fig. 3-2.** Conformational changes of peptide (LK)<sub>8</sub>-vinyl depend on concentration.

increasing the local concentration of the graft peptide induces intermolecular hydrogen bonding and the formation of a  $\beta$ -sheet structure. The CD spectra of LKNIPAm could not be fitted by a linear combination of typical CD spectra for dispersed  $\alpha$ -helix,  $\beta$ -sheet, and random coil conformations. Fig. 3-3 shows the pH dependence of the molar ellipticity at 218 nm,  $[\theta]_{218\text{nm}}$ , assigned to the  $\beta$ -sheet structure for LKNIPAm in aqueous solution, as the pH of the solution was increased (○) or decreased (●). A large hysteresis was observed in the pH-induced conformational transition of the (Leu-Lys)<sub>8</sub> graft chains in LKNIPAm. This result implies that the rate of the conformational transition from stable  $\beta$ -sheet to

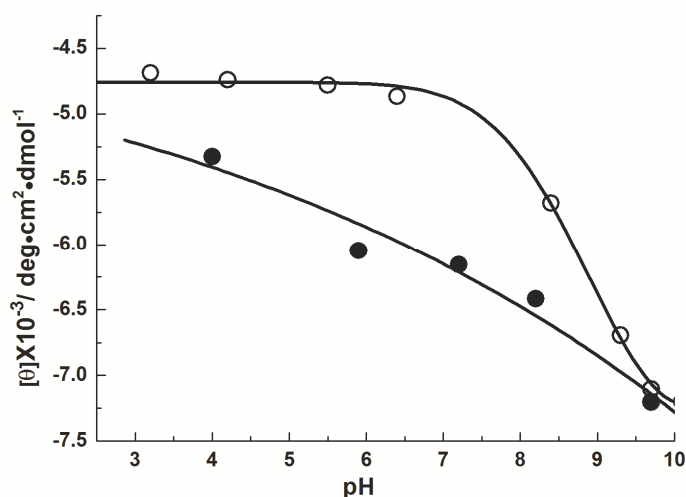


**Fig. 3-3.** pH dependence of the molar ellipticity at 218 nm,  $[\theta]_{218\text{nm}}$ , for LKNIPAm in aqueous solution, when the pH of the solution was increased (○) and decreased (●).

random coil was slower than that of random coil to  $\beta$ -sheet, comparing to the case of the free (Leu-Lys)<sub>8</sub>-vinyl (Fig. 3-2).

### 3-3-2 pH- and thermo- complex induced conformational changes of LKNIPAm

The conformation of (Leu-Lys)<sub>8</sub>-vinyl did not change with the temperature (from 10 to 45 °C) under acidic or basic conditions. In this research, we chose PNIPAm as the thermo-responsive part of the multi-stimuli responsive copolymer. We investigated the thermo-induced turbidity changes owing to the coil-to-globule transition of the main chain in LKNIPAm by the transmittance at 450 nm in aqueous solution. Fig. 3-4 shows the thermo-induced transmittance changes at 450 nm of the LKNIPAm aqueous solution at pH 3.0 (Fig. 3-4a) and pH 9.0 (Fig. 3-4b). At pH 3.0, the transmittance at 450 nm did not change and remained relatively high. However, at pH 9.0, the transmittance drastically increased with increasing temperature, beginning at approximately 37 °C. In this case, LKNIPAm partially precipitated above 40 °C. We also investigated the thermo-induced conformational changes of the (Leu-Lys)<sub>8</sub> graft chain in LKNIPAm at 25 °C and 40 °C by FT-IR measurements. The samples for the FT-IR measurements were prepared as follows. The pH and temperature of LKNIPAm aqueous solution were adjusted to the desired values (pH 3.0, pH 9.0,



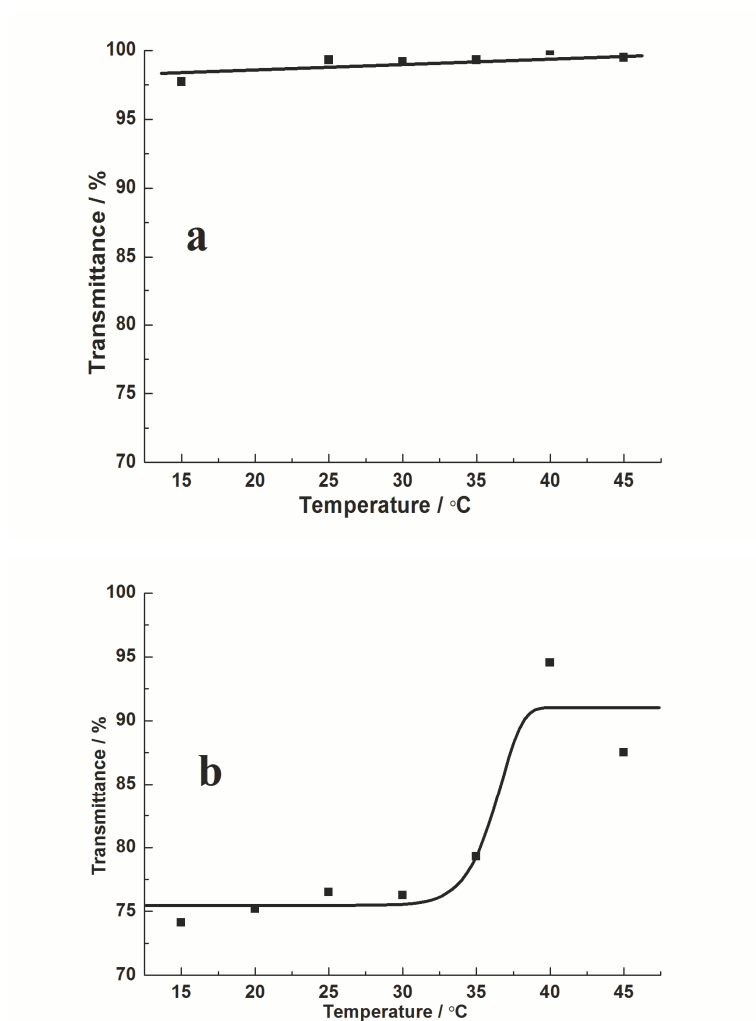


**Fig. 3-4.** Thermo-induced transmittance changes at 450 nm of LKNIPAm aqueous solution at (a) pH 3.0 and (b) pH 9.0, respectively.

25 °C, 40 °C). The LKNIPAm solutions were quickly frozen in liquid nitrogen and lyophilized to obtain measurement samples. Beforehand, we verified that no conformational changes had occurred during the lyophilization process. The secondary structure of the water-soluble peptide in aqueous solution was measured by CD. The fraction of the second-order structure obtained by the FT-IR measurement of the lyophilized peptide was in fair agreement with that obtained by the CD measurement in aqueous solution. Fig. 3-5 shows the pH- and thermo-induced FT-IR spectra of LKNIPAm. In the spectra, characteristic absorptions of the amide I band in  $\alpha$ -helix,  $\beta$ -sheet, and random coil conformations were observed at 1650, 1630, and 1675  $\text{cm}^{-1}$ , respectively<sup>19</sup>. The ratio of the integrated peak intensities assigned to the

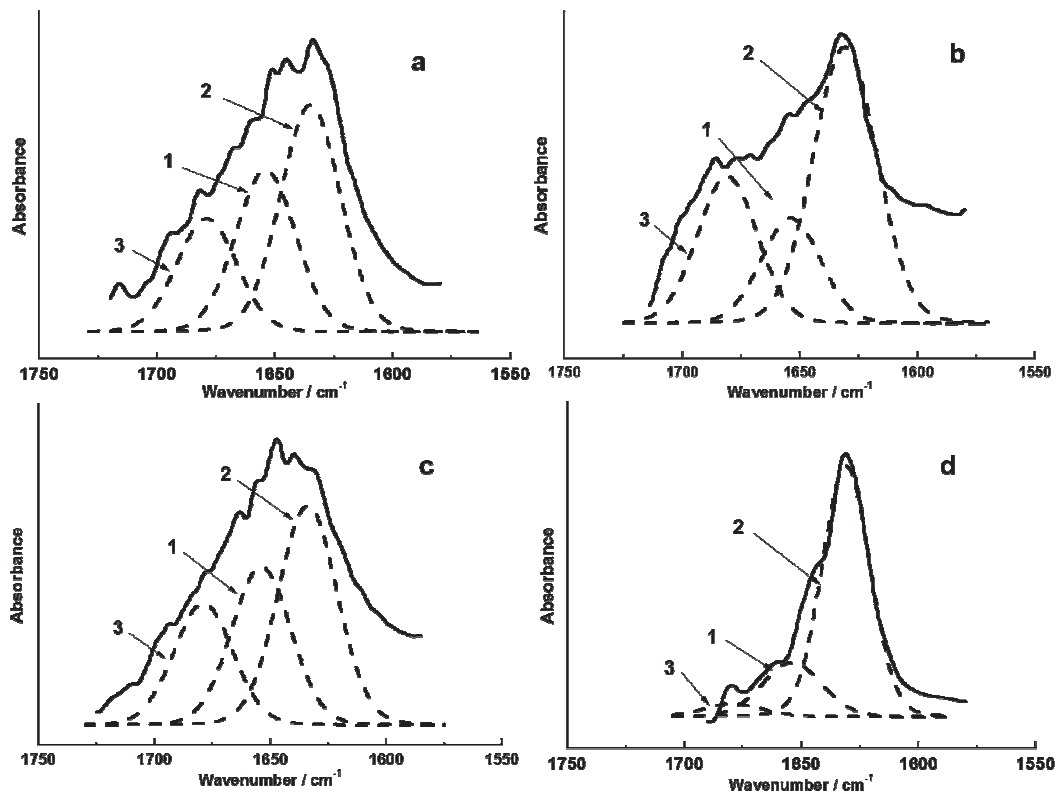


**Fig. 3-5.** FT-IR spectra of LKNIPAm prepared quickly frozen and lyophilized at a) pH 3.0, 25 °C; b) pH 3.0, 40 °C; c) pH 9.0, 25 °C; and d) pH 9.0, 40 °C respectively. Broken lines show the peak deconvolution of the amide I band to (1)  $\alpha$ -helix, (2)  $\beta$ -sheet, and (3) random coil conformations.

individual secondary structures, which was obtained by peak deconvolution of the amide I band, gave the percentage of the different conformations of the  $(\text{Leu-Lys})_8$  graft chain in LKNIPAm. The results of the conformational analysis are summarized in Table 3-1. Stable  $\beta$ -sheet structure formation among the  $(\text{Leu-Lys})_8$  graft chains occurred only under basic conditions at high temperature (pH 9.0 and 40 °C). The observed pH- and thermo-induced conformational transition of LKNIPAm in aqueous solution could be explained as follows. Under acidic conditions (pH 3.0), the  $(\text{Leu-Lys})_8$  graft chain of LKNIPAm was protonated and positively charged. The ionized graft peptides increased the water solubility of LKNIPAm at high temperatures, where the PNIPAm main chain forms a globular conformation. Meanwhile, under basic conditions (pH 9.0), the  $(\text{Leu-Lys})_8$  graft peptides were neutral. At low temperatures, the PNIPAm main chain forms a coil conformation. The conformation of the main chain of LKNIPAm disturbed the  $\beta$ -sheet formation of the

**Table 3-1.** The fractions of the second order structure of (Leu-Lys)<sub>8</sub> graft chain in LKNIPAm.

pH	Temperature / °C	Conformation / %		
		$\alpha$ -helix	$\beta$ -sheet	random coil
3.0	25	36	40	24
	40	23	46	31
9.0	25	31	45	24
	40	20	75	5

peptide graft chain. The hydrophobic interactions among the peptide graft chains resulted in the formation of a micellar structure. The formation of these LKNIPAm micelles induced the decrease of the transmittance at 450 nm. At high temperatures (40 °C), the PNIPAm main chain formed a globular conformation. Under these conditions, the grafted peptide chains formed a  $\beta$ -sheet conformation. The  $\beta$ -sheet structure of the peptide graft chains acted as bridging points among the LKNIPAm micelles, resulting in

precipitation. Fig. 3-6 was the photos of LKNIPAm solved in water under various pH conditions. It is clearly showed in this figure that the polymer

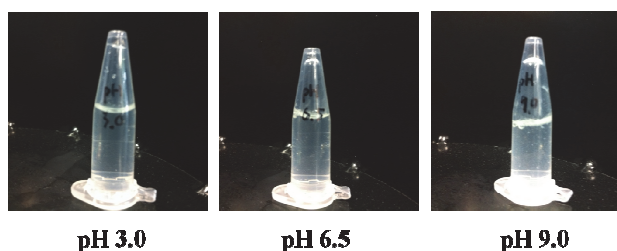


**Fig. 3-6.** Photos of the polymer solution under various pH at 20 °C.

solution was transparent at pH 3.0 and pH 6.5. However, at pH 9.0, the polymer did not completely dissolved in aqueous solution and the solution was turbid. This phenomenon proved the explanation that under the basic condition the intermolecular  $\beta$ -sheet structure performed as bridge linked the PNIPAm chains. And this led to the formation of polymer aggregations which reduced the solubility of the peptide grafted polymer.

### 3-3-3 pH- and thermo-induced morphological changes of LKNIPAm in aqueous solution

The pH- and thermo-induced morphological changes of LKNIPAm owing to the

conformational transitions of the main chain (PNIPAm) and peptide graft chains (Leu-Lys)<sub>8</sub> in aqueous solution were observed directly with a transmission electron microscope using a freeze-fracture-etching replica technique. The LKNIPAm aqueous solution at the desired pH and temperature were quickly frozen, and then the replicas were prepared by the freeze-fracture-etching technique. Fig. 3-7 shows the TEM images of LKNIPAm in aqueous solution. Under acidic conditions (pH 3.0), the

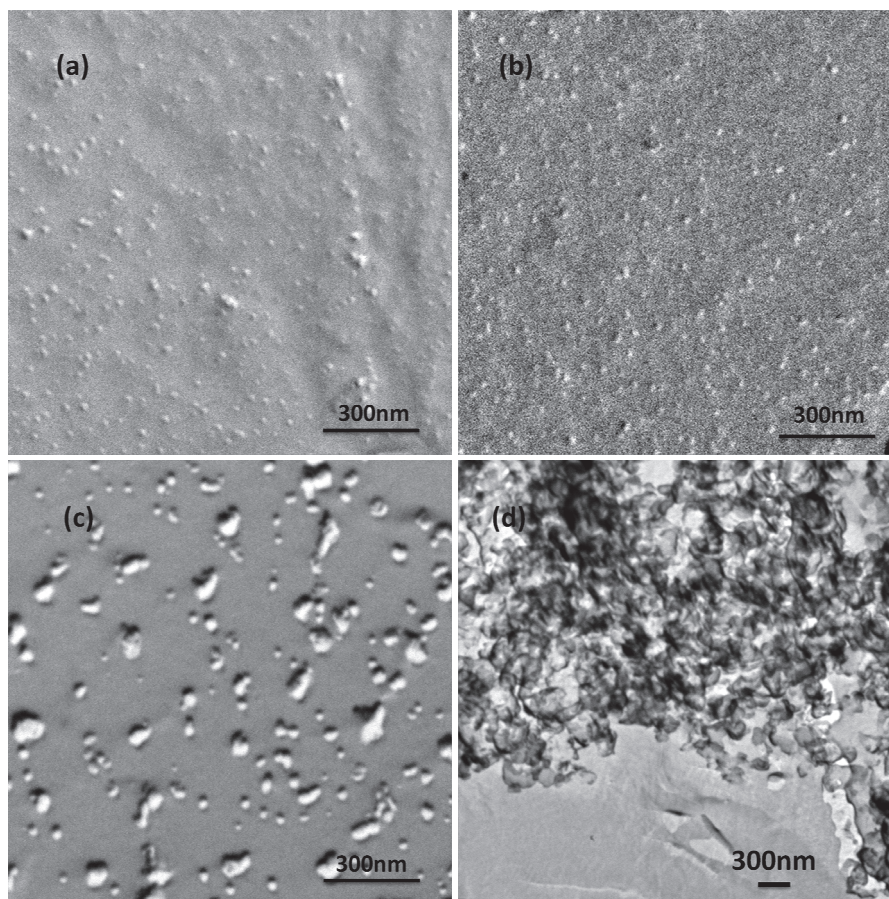


**Fig. 3-7.** pH- and thermo- induced morphological changes of LKNIPAm in aqueous solution observed by TEM using freeze-fracture-etching technique at a) pH 3.0, 25 °C, b) pH 3.0, 40 °C, c) pH 9.0, 25 °C, d) pH 9.0, 40 °C respectively.

(Leu-Lys)<sub>8</sub> graft chain of LKNIPAm was positively charged and took a random coil and  $\alpha$ -helical conformation with a considerable amount of  $\beta$ -sheet structure (Fig. 3-5a and 3-5b). At the low temperature of 25 °C, below the coil-to-globule transition temperature, the main chain of LKNIPAm formed a coil conformation. Under these conditions, LKNIPAm formed water-soluble nanoparticles, in which the partially formed  $\beta$ -sheet structure of the grafted peptides bridged the main chains of LKNIPAm.

In Fig. 3-7a, nanoparticles with a diameter of 3 nm - 45 nm were observed. By increasing the temperature to 40 °C, above the coil-to-globule transition temperature, the PNIPAm main chain adopted a shrunken globule form. However, the (Leu-Lys)<sub>8</sub> graft chains of the LKNIPAm were charged, and the formation of the  $\beta$ -sheet structure was disturbed by the electrostatic repulsion between the graft chains. The morphology of the LKNIPAm in this case was a maintained dispersed particle with a diameter of 10 nm - 60 nm (Fig. 3-7b). In basic solution (pH 9.0) and at low temperature (25 °C), LKNIPAm formed relatively larger particles compared to those formed under acidic conditions (Fig. 3-7c, diameter 30 nm – 150 nm). In this case, the PNIPAm main chain took on a water-soluble coil conformation, and the peptide graft chains were neutral. However, the formation of the  $\beta$ -sheet structure that acted as a bridging point between the LKNIPAm polymer strands was disturbed by the expanded flexible coil conformation of the PNIPAm main chain. These effects resulted in the formation of relatively large dispersed particles. At the higher temperature of 40 °C, PNIPAm adopted a shrunken globule conformation, and the (Leu-Lys)<sub>8</sub> graft chains formed a stable  $\beta$ -sheet structure (Fig. 3-7d). Fig. 3-7d shows the LKNIPAm morphology at pH 9.0 and 40 °C in aqueous solution. In this image, a large aggregate can be observed. This aggregated body was formed by the cross-linking of LKNIPAm, whose main chain was a shrunken globule, through the formation of bridging  $\beta$ -sheets of the grafted peptide chains.

### **3-4 Photo-initiated Peptide Grafted PNIPAm**

#### **3-4-1 Preparation of Peptide Grafted Copolymer**

Because of the environmental friendly requirement, we also synthesized the peptide grafted PNIPAm by photo polymerization. (Leu-Lys)<sub>8</sub>-vinyl (20 mg) and NIPAm (4.5 mg) were dissolved in aqueous solution. The oxygen was removed through three freeze-pump-thaw cycles. The copolymerization of the (Leu-Lys)<sub>8</sub>-vinyl and NIPAm was initiated by water soluble photoinitiator 2-Hydroxy-4'-(2-hydroxyethoxy)-2-methylpropiophenone (photocure 2959) under the

UV irradiation for 1h. The products were dissolved in water, and the aqueous solution was dialyzed against water using a molecular porous membrane tube. After the dialysis, the solution was lyophilized to obtain LKNIPAm. The graft peptide content of 27.2 mol% in LKNIPAm was estimated by means of  $^1\text{H-NMR}$  spectroscopy in deuterated TFA, on the basis of the area ratio of the signals same as before. We could find that the peptide content was higher than thermal-initiated because of the high initiation efficiency and homogeneous phase of the monomer solution.

### 3-4-2 Characterization of Photo-initiated Copolymer

The photo-initiated peptide grafted PNIPAm was characterized by the CD spectrum to characterize the conformational changes induced by pH, and the morphology changes were observed by the transmission electron microscope.

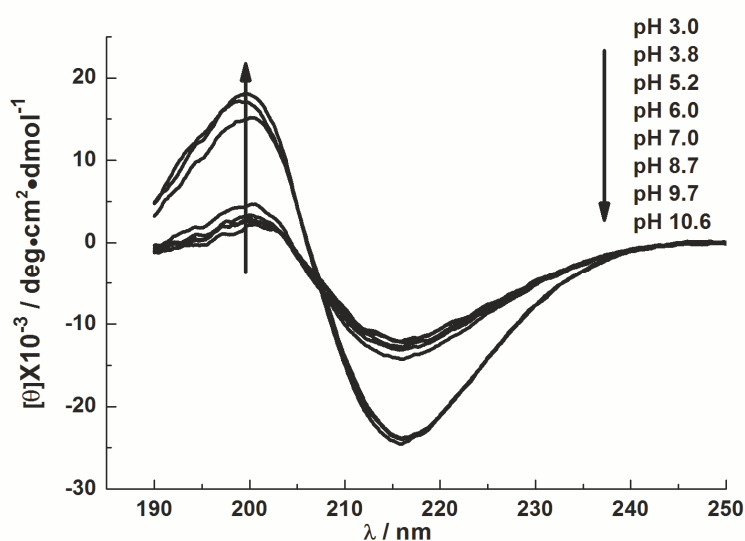


**Fig. 3-8.** pH-induced CD spectral changes of photoinitiated LKNIPAm in aqueous solution as pH increased.

The conformational changes of photoinitiated LKNIPAm was exhibited in Fig. 3-8. The conformational changes of peptide chains seem similar to the thermal initiated polymer. The negative peak at 218 nm indicated the  $\beta$ -sheet structure. The molar ellipticity at 218 nm increased with the increasing of pH, this means the  $\beta$ -sheet structure of peptide graft chain was increased as pH increased. Especially when pH changes from acidic to basic condition, the  $\beta$ -sheet content had a dramatically



increase because of the coil to  $\beta$ -sheet transition of peptide (LK)<sub>8</sub>.

TEM images under pH 3.0 and pH 9.0 at 20 °C were showed in Fig. 3-9. The polymer formed small particles at pH 3.0 (Fig. 3-9a) and the morphology of polymer

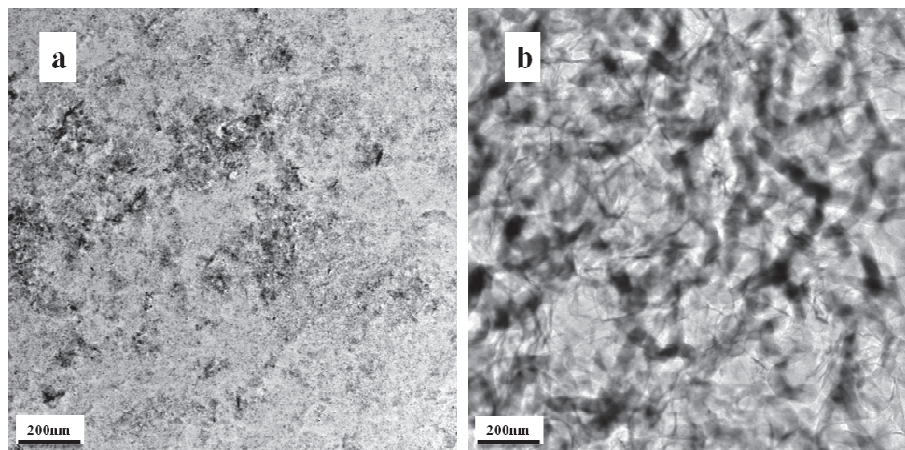


**Fig. 3-9.** TEM images photo-initiated (LK)<sub>8</sub> grafted PNIPAm under pH 3.0 (a) and pH 9.0 (b) at 20 °C.

transformed to fiber structure at pH 9.0 (Fig. 3-9b), which was formed by the  $\beta$ -sheet structure assembly. From these simple characterization, we believe that the polymerization method did not influence the properties of the peptide grafted PNIPAm.

### 3-5 Conclusions

In conclusion, the amphiphilic copolymer, (Leu-Lys)<sub>8</sub>-grafted poly(*N*-isopropylacrylamide), shows pH- and thermo-induced conformational and morphological transitions in aqueous solution. Schematic pictures of the proposed pH- and thermo-induced structural changes of LKNIPAm are illustrated in Fig. 3-10. Under acidic conditions, the peptide graft chains were protonated and positively charged, and LKNIPAm formed nanoparticles owing to the electrostatic repulsion among the graft chains above and below the coil-to-globule transition temperature of the PNIPAm main chain. However, under basic conditions, the peptide graft chains were neutral, and at low temperature below the transition temperature of the main

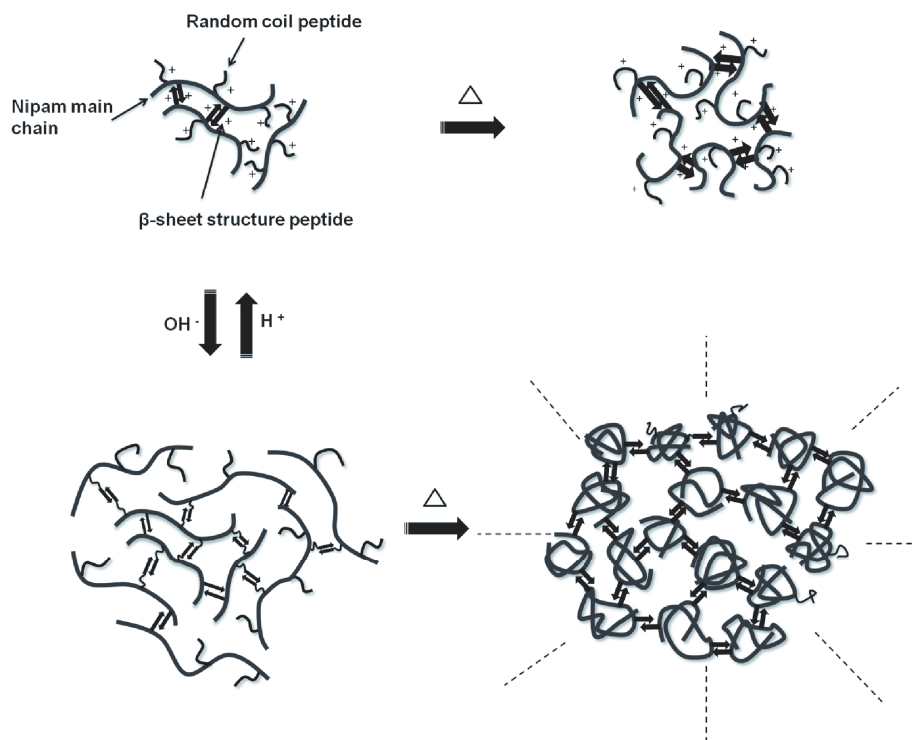


**Fig. 3-9.** Schematic picture of pH- and thermo- induced structural changes of LKNIPAm in aqueous solution.

chain, LKNIPAm formed a micellar structure. Only at high temperature above the transition temperature, in which the main chain formed shrunken globules, did the peptide graft chains form a stable  $\beta$ -sheet structure. The  $\beta$ -sheets of the grafted chains acted as bridging points between the LKNIPAm globules, resulting in the formation of a large aggregated body.

We believe that these studies of the structural regulation of multi-stimuli responsive polymers provide useful information for the development of novel stimuli-responsive materials with a wide range of applications in nanotechnology. Because of environmental friendly and high initiation efficiency, we chose photopolymerization to synthesis the polymers for the investigation of further applications.

## Reference

1. Eun Seok Gil&Samuel M. Hudson, Stimuli-reponsive polymers and their bioconjugates, *Progress in Polymer Science*. **29**, 1173-1222 (2004).



2. Younsoo Bae, Shigeto Fukushima, Atsushi Harada & Kazunori Kataoka, Design of Environment-Sensitive Supramolecular Assemblies for Intracellular Drug Delivery: Polymeric Micelles that are Responsive to Intracellular pH Change, *Angewandte Chemie International Edition*. **42**, 4640-4643 (2003).
3. Mirko Nitschke, Stefan Gramm, Thomas Götze, Monika Valtink, Juliane Drichel, Brigitte Voit, Katrin Engelmann & Carsten Werner, Thermo-responsive poly(NiPAAm-co-DEGMA) substrates for gentle harvest of human corneal endothelial cell sheets, *Journal of Biomedical Materials Research Part A*. **80A**, 1003-1010 (2007).
4. Mary A. Reppy & Bradford A. Pindzola, Biosensing with polydiacetylene materials: structures, optical properties and applications, *Chemical Communications*. 4317-4338 (2007).
5. Yoichi Tachibana, Motoichi Kurisawa, Hiroshi Uyama & Shiro Kobayashi, Thermo- and pH-Responsive Biodegradable Poly( $\alpha$ -N-substituted  $\gamma$ -glutamine)s, *Biomacromolecules*. **4**, 1132-1134 (2003).
6. Yuanli Cai, Yiqing Tang & Steven P. Armes, Direct Synthesis and Stimulus-Responsive Micellization of Y-Shaped Hydrophilic Block Copolymers, *Macromolecules*. **37**, 9728-9737 (2004).
7. Frederic Eeckman, André J. Moës & Karim Amighi, Synthesis and characterization of thermosensitive copolymers for oral controlled drug delivery, *European Polymer Journal*. **40**, 873-881 (2004).
8. Sivanand S. Pennadam, Matthieu D. Lavigne, Christina F. Dutta, Keith Firman, Darren Mernagh, Dariusz C. Górecki & Cameron Alexander, Control of A Multisubunit DNA Motor by a Thermoresponsive Polymer Switch, *Journal of the American Chemical Society*. **126**, 13208-13209 (2004).
9. Taichi Ito, Takanobu Hioki, Takeo Yamaguchi, Toshio Shinbo, Shin-ichi Nakao & Shoji Kimura, Development of a Molecular Recognition Ion Gating Membrane and Estimation of Its Pore Size Control, *Journal of the American Chemical Society*. **124**, 7840-7846 (2002).
10. Katharina Janek, Joachim Behlke, Josef Zipper, Heinz Fabian, Yannis Georgalis, Michael Beyermann, Michael Bienert & Eberhard Krause, Water-Soluble  $\beta$ -Sheet Models Which Self-Assemble into Fibrillar Structures†, *Biochemistry*. **38**, 8246-8252 (1999).
11. Peter T. Lansbury, A Reductionist View of Alzheimer's Disease, *Accounts of Chemical*

*Research*. **29**, 317-321 (1996).

12. Tomoyuki Koga, Kazuhiro Taguchi, Takatoshi Kinoshita & Masahiro Higuchi, pH-Regulated formation of amyloid-like [small beta]-sheet assemblies from polyglutamate grafted polyallylamine, *Chemical Communications*. 242-243 (2002).
13. Tomoyuki Koga, Kazuhiro Taguchi, Yoshiaki Kobuke, Takatoshi Kinoshita & Masahiro Higuchi, Structural Regulation of a Peptide-Conjugated Graft Copolymer: A Simple Model for Amyloid Formation, *Chemistry – A European Journal*. **9**, 1146-1156 (2003).
14. Tomoyuki Koga, Kazuhiro Taguchi, Masaki Kogiso, Yoshiaki Kobuke, Takatoshi Kinoshita & Masahiro Higuchi, Amyloid formation of native folded protein induced by peptide-based graft copolymer, *FEBS letters*. **531**, 137-140 (2002).
15. Takateru Inoue Masahiro Higuchi, Hidenori Miyashi, Masami Kawaguchi, pH-Induced Reversible Conformational and Morphological Regulation of Poly-leucine Grafted Polyallylamine Assembly in Solution, *Langmuir*. **21**, 11462-11467 (2005).
16. Barbara Trzebicka, Barbara Robak, Roza Trzcinska, Dawid Szweda, Piotr Suder, Jerzy Silberring & Andrzej Dworak, Thermosensitive PNIPAM-peptide conjugate – Synthesis and aggregation, *European Polymer Journal*. **49**, 499-509 (2013).
17. Mary Jo Turk, Joseph A. Reddy, Jean A. Chmielewski & Philip S. Low, Characterization of a novel pH-sensitive peptide that enhances drug release from folate-targeted liposomes at endosomal pHs, *Biochimica et Biophysica Acta (BBA) - Biomembranes*. **1559**, 56-68 (2002).
18. Chaoxu Li, Mohammad M. Alam, Sreenath Bolisetty, Jozef Adamcik & Raffaele Mezzenga, New biocompatible thermo-reversible hydrogels from PNIPAM-decorated amyloid fibrils, *Chemical Communications*. **47**, 2913-2915 (2011).
19. T. Miyazawa & E. R. Blout, The Infrared Spectra of Polypeptides in Various Conformations: Amide I and II Bands, *Journal of the American Chemical Society*. **83**, 712-719 (1961).

## Chapter 4

# **pH- and Thermo-induced Specific Permeability of Chiral Amino Acids through the Peptide Grafted Poly(N-isopropylamide) Network Membrane**

### **4-1 Introduction**

Chirality plays an important role in the function of biological processes. The different enantiomers of a chiral drug usually exhibit different pharmacological activities, metabolic effects, metabolic rates, and toxicities due to the high degree of stereoselectivity<sup>1-3</sup>. In some cases, only one of the enantiomers of a chiral drug contributes to its pharmacodynamic behavior, while the other shows no or a much weaker effect as well as side-effects or even toxicity<sup>4</sup>. Besides the use of single enantiomers in the pharmaceutical industry, enantiomerically pure compounds are becoming significant in the production of other chemical products increasingly, such as agrochemicals, fragrances, and foods.<sup>5</sup> Currently, separation of racemic mixtures is typically performed by column chromatography<sup>6</sup>, preferential crystallization<sup>7</sup> or kinetic resolution<sup>8</sup>. These methods have various advantages but also disadvantages, including high energy consumption, high cost, low efficiency, and discontinuous operation. Low-cost, continuous, high-efficiency separation technology is clearly needed for commercial-scale preparation of enantiomerically pure substances. Membrane technology, fortunately, fulfils this need very well because of its high efficiency, low energy usage, simplicity, convenience for up- and/or downscaling, and continuous operability. Enantioselective membranes include liquid membranes and solid membranes that can achieve enantioseparation by binding the two enantiomers with different affinities. Solid membranes are usually long-term stable because of self-supporting structure or attached on base membranes<sup>9</sup>. Among solid membranes, polymer membranes containing amino acid have widely studied<sup>10-13</sup>. But these membrane systems were not responsive to external stimuli. In our previous studies<sup>14</sup>,

we have reported a functional molecular membrane composed of peptide which is sensitive to pH conditions.

Poly (*N*-isopropylacrylamide) (PNIPAm) and its copolymers is the most extensively studied thermo-sensitive polymer, which exhibit a lower critical solution temperature (LCST) in aqueous solution. PNIPAm chains hydrate to form expanded structures in water when the temperature is below its LCST, but become compact structures by dehydration when heated above its LCST. The volume-phase transition brings about drastic changes in the physical properties of the PNIPAm gels.

Photopolymerization has its own particular advantages<sup>15</sup>. The most substantial advantage is that the photochemical process is extremely fast, and no volatile organic compounds are released in this process. Low activation energy is another advantage of photochemical initiation; it is possible to perform photopolymerization at or below room temperature<sup>16,17</sup>. For all these reasons, photopolymerization represents an ecological alternative to the thermal process. In this research, according to our previous work we synthesized a membrane consisting of a PNIPAm network with peptide graft chains and porous support membrane by photo-initiated polymerization. The membrane has pH and thermo-responsiveness. The pH and thermo-response in the permeability and permselectivity of peptides is investigated.

## **4-2 Experimental Section**

### **4-2-1 Materials**

*N*-isopropylamide (NIPAm, TCI, Tokyo, Japan) was purified by recrystallization from hexane. *N,N'*-methylenebisacrylamide (BisAAM, Nacalai tesque, Kyoto, Japan) and 2-Hydroxy-4'-(2-hydroxyethoxy)-2-methylpropiophenone (photocure 2959, Aldrich, USA) were used without purification. Ultrapure water with a conductivity of 18  $\mu\text{S cm}^{-1}$  was used in all experiments. MF-millipore membrane filter (MF, thickness 180  $\mu\text{m}$ , pore size 0.22  $\mu\text{m}$ , porosity 75%, Millipore, USA) was used as a porous supported membrane.

#### 4-2-2 Preparation of polymer membrane

The peptide ( $L$ -Leu- $L$ -Lys) $_8$ -vinyl ((LK) $_8$ -vinyl) was synthesized by the way that we reported<sup>18</sup>. The typical procedure for photopolymerization was used; 10 mg of NIPAm, 20 mg of (LK) $_8$ -vinyl, and 1.5 mg (and 0.5 mg) of BisAA as a cross-linker were dissolved in 1 ml of water and stirred in a 10 ml flask at room temperature. Then 100  $\mu$ L acetone solution of photoinitiator (containing 2959 2mg) was added into the monomer solution. Freeze-deaeration was carried out three times to remove the oxygen. The MF membrane was immersed in the reaction mixture to impregnate the monomer solution in the pore of the membrane. After this process, the membrane was took out from the solution and put on a Teflon dish in glove box. The polymerization was occurred by UV irradiation for 2h. After the polymerization, the membrane was immersed in the pure water to remove the unreacted monomer and the crosslinking agent. From the elemental analysis of the two crosslinked membranes, we obtained the contents of the peptide graft chain and the crosslinker. The graft content of the both membranes was 4 mol%. The crosslinking degrees of the membranes were 1.5% (low-crosslinked) and 16% (high-crosslinked), respectively.

#### 4-2-3 Characterization of the peptide grafted membrane

In this research, we synthesized the membrane without the porous support membrane at the same condition to characterize the degree of hydration and elongation, composition, pKa and conformation of the peptide graft chains in membrane. The synthesized polymer without MF membrane was dried in vacuum drier for 2 days.

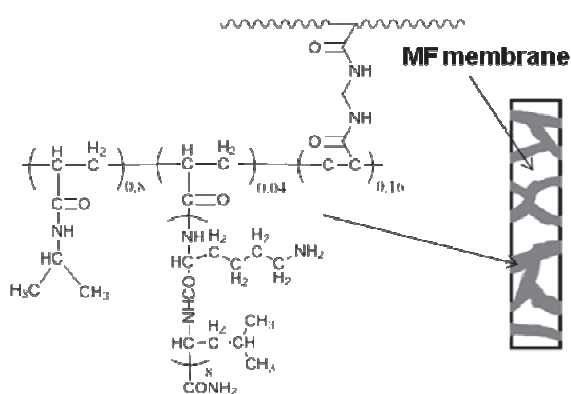


**Fig. 4-1.** Schematic picture of the peptide grafted PNIPAm network membrane and the chemical structure of the crosslinked polymer.

From the element analysis we calculated the molar ratio of NIPAm; 0.8, peptide graft chain; 0.04, cross linker; 0.16, respectively. The schematic picture of the membrane

was showed in Fig. 4-1. The pKa of the amino group of the lysine residues in the membrane was determined to be 7.5 by the pH titration.

We think that the permeability through the peptide grafted PNIPAm network membrane was influenced by the conformation of peptide graft chains and PNIPAm main chain. The degree of hydration and elongation of the membrane are sensitive to the structural changes of the PNIPAm main chain and peptide graft chains. Here we use the water content of swollen membrane indicated the degree of hydration of the membrane. The equation to calculate the degree of hydration of the membrane ( $H$ ) is as follows:  $H = (M_s - M_0) / M_s$ , where  $M_s$  is the weight of swollen membrane and  $M_0$  is the weight of dried membrane. The elongation of the membrane was characterized by the USB microscope (M2, Scalar, Tokyo, Japan). The degree of elongation of the membrane under the several conditions was obtained from the changing in the length of the membrane. The degree of elongation value,  $L$ , was calculated as follows;  $L = L_m / L_0$ , where  $L_m$  is the length that measured under the several conditions and  $L_0$  is the length of the membrane dipped in aqueous solution at pH 6.5 and 20 °C as a standard value. The membrane was swollen in the aqueous solution under the several conditions (pH and temperature), blotted, and weighed and measured repeatedly until a constant weight and length were obtained. The results of hydration and elongation were listed in Table 4-1.

#### **4-2-4 FT-IR measurements**

Secondary structural changes of the peptide graft chains in the polymer membrane were estimated by Transmittance Fourier transform infrared (TM-FTIR) spectroscopy. The TM-FTIR spectra were measured with a Perkin-Elmer Spectra 2000 (resolution: 4  $\text{cm}^{-1}$ , number of scan: 32). The membranes were dipped in aqueous solutions at various conditions (pH and temperature) and quickly frozen in liquid nitrogen, and then the frozen samples were lyophilized to obtain the dried membrane powder. The pellets for TM-FTIR measurements were prepared by the mixing of the membrane powder and KBr. The weight fraction of the membrane was fixed at 1 wt%.

#### 4-2-5 Permeability measurements

The permeability measurements of the phenylalanine through the membrane were carried out with a Pyrex glass permeation cell. The membrane was placed between the two parts of the cells pressed by two pieces of Millipore supported membrane to form the sandwich structure. A 5 mM aqueous solution of L-phenylalanine or D-phenylalanine was introduced into one side of the cell, and phenylalanine free water was into the other side (the permeated side) of the cell. The pH of the both solution in the cell was adjusted with 0.1 M HCl or 0.1 M NaOH. The changes in the phenylalanine concentration with time on the permeated side was measured with an UV-vis spectrophotometer (UV-3600, Shimadzu, Japan), from the absorbance at 256.5 nm on the basis of the molar extinction coefficient of the phenylalanine. Fig. 4-2 shows a typical example of the time-dependent changes of the L- and D- phenylalanine concentration on the permeation side at 20 °C and pH 6.5, respectively. From the initial slopes of the curves of Fig. 4-2 (denoted by the dotted lines), the fluxes

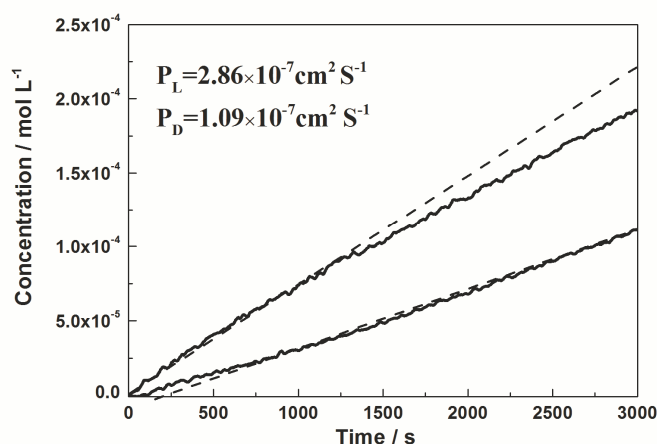


**Fig. 4-2.** Permeation curve for L- and D- phenylalanine through the peptide grafted PNIPAM crosslinked membrane at 20 °C and pH 6.5.

of L- and D- phenylalanine [ $J$  ( $\text{mol}^{-1} \text{cm}^{-2} \text{s}^{-1}$ )] through the membrane was calculated. The permeate coefficients  $P$  ( $\text{cm}^2 \text{s}^{-1}$ ) of L- and D- phenylalanine were calculated by the equation as follow;  $P = J \cdot \delta / \Delta c$ , where  $\delta$  is the membrane thickness and  $\Delta c$  is the external concentration difference of L- or D- phenylalanine across the membrane. In this study, the membrane area was the area of the swollen polymer incorporated domain in the MF-membrane for an effective permeation area. The permeability

measurements of the L- or D- phenylalanine were performed 3 times under the same condition, and the  $P$  values for the L- and D- phenylalanine were obtained as an averaged value,  $P_L$  and  $P_D$ , respectively. The permselectivity,  $\alpha$ , of L-phenylalanine to D-phenylalanine through the membrane was obtained as follows;  $\alpha = P_L / P_D$ .

## 4-3 Result and Discussion

### 4-3-1 Degree of hydration and elongation of the membrane affected by external conditions

In this research, the main component of the membrane is PNIPAm, which was introduced to give the thermal sensitive property for this polymer membrane. PNIPAm gels have well swollen ability and it is known that the gels shrink above 32 °C in water<sup>19</sup>. Hydration degrees of the membrane under different conditions were shown in Table 4-1.

**Table 4-1** The degree of hydration and elongation of the polymer membrane under different conditions

pH	T / °C	H / %	L / %
3.0	20	96.8	95.8
	40	96.5	92.1
6.5	20	98.2	100
	40	97.8	96.9
9.0	20	96.8	80.9
	40	96.3	77.1

The degree of hydration reached maximum 98.2% at pH 6.5 and 20 °C. This is mainly because of the hydration of the PNIPAm main chains. At 20 °C, the PNIPAm was hydration and formed expanded structure. But when temperature increased to 40 °C, which is higher than the LCST temperature of PNIPAm, the PNIPAm formed compact structures by dehydration<sup>20</sup>. The crosslinking degree of the membrane was relatively high (BisAA content was 16%). The conformational transition of the PNIPAm main chain was disturbed and the membrane trapped the water, resulted in



the relatively high water content. However, at pH 3.0 and pH 9.0, the degree of the hydration slightly decreased compared with that under neutral pH condition. Under the acidic condition, pH 3.0, the peptide graft chains were protonated. The ionized amino groups of the Lys residues that exist in the vicinity of the PNIPAM main chains, disturbed the hydration of the polar parts of the PNIPAM by the ionic effect<sup>21,22</sup>. On the other hand, under the basic condition, pH 9.0, hydrophobic interaction among the deprotonated peptide graft chains induced the relatively lower hydration of the PNIPAM main chain. The degree of the elongation of the membrane showed same tendency (Table 1). At the high temperature, 40 °C, above the LCST, the PNIPAM main chains were dehydrations and led to the shrunk of the membrane. Especially, the degree of elongation of the membrane was clearly decreased under the basic condition (pH 9.0). Under this condition, the peptide graft chains were deprotonated and the hydrophobic interaction among the peptide graft chains induced the membrane shrinking. Furthermore, this membrane shrinking was remarkable at 40 °C because of the conformational transition of the PNIPAM main chains and the hydrophobic interaction among the peptide graft chains.

#### **4-3-2 pH-induced conformational transition of the peptides graft chain in the membrane**

We investigated the conformational changes of the peptide graft chains in the membrane at 20 °C and 40 °C by the TM-FTIR measurements. The samples for TM-FTIR measurements were prepared as follows, the polymer membrane was dipped in the aqueous solutions, which was adjusted at designed pH and temperature. The solutions contained membrane were quickly frozen in liquid nitrogen and lyophilized to obtain measurement samples. Beforehand we checked that the conformational changes did not occur during the lyophilization process. Fig. 4-3 shows the TM-FTIR absorption spectra of the polymer membranes under various conditions. In the spectra, characteristic absorptions of the amide I band with  $\alpha$ -helix,  $\beta$ -sheet, and random coil conformations were observed at 1650, 1630, and 1675  $\text{cm}^{-1}$ ,

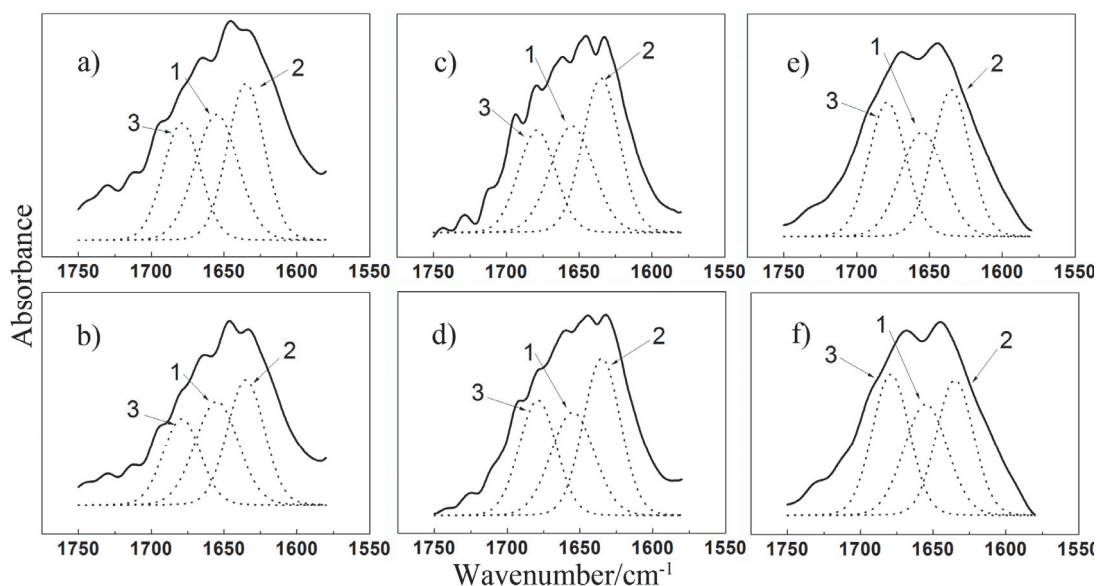


**Fig. 4-3.** TM-FTIR spectra of peptide graft chains in the PNIPAm membrane prepared by quickly frozen and lyophilized at a) pH 3.0, 20 °C; b) pH 3.0, 40 °C; c) pH 6.5, 20 °C; d) pH 6.5, 40 °C; e) pH 9.0, 20 °C ; and f) pH 9.0, 40 °C respectively. Broken lines show the peak deconvolution of the amide I band to 1;  $\alpha$ -helix, 2;  $\beta$ -sheet, and 3; random coil conformations.

respectively<sup>12</sup>. The ratio of integrated peak intensities assigned to individual secondary structure, which was obtained by peak deconvolution of the amide I band, gave the percentage of conformational changes of the peptide graft chain in the membrane. The results of conformational analysis were summarized in Table 4-2. From this table, we could found that temperature had little effect on the conformational changes of the peptide graft chain. The composition of secondary

**Table 4-2** Thermo- and pH- induced conformation changes of the peptide graft chain in the PNIPAm membrane.

pH	T / °C	conformation		
		$\alpha$ -helix / %	$\beta$ -sheet / %	random coil / %
3.0	20	34.9	37.2	27.9
	40	36.4	37.7	25.9
6.5	20	33.3	39.2	27.5
	40	30.7	40.0	29.3
9.0	20	30.3	36.4	33.3
	40	30.6	36.1	33.3

structure was merely not changed when the temperature increased from 20 °C to 40 °C. At pH 6.5, the content of  $\beta$ -sheet structure was slightly higher than that under the acidic and basic conditions. This could be explained as follows; under the acidic condition, pH 3.0, the inter-molecular hydrogen bonding to form the  $\beta$ -sheet structure among the protonated peptide graft chains was disturbed owing to the electrostatic repulsion. Under the basic condition, pH 9.0, the deprotonated peptide chains aggregated rapidly owing to the hydrophobic interaction. The aggregation disturbed the formation of regular structure, and resulted in the increasing of the random coil conformation.

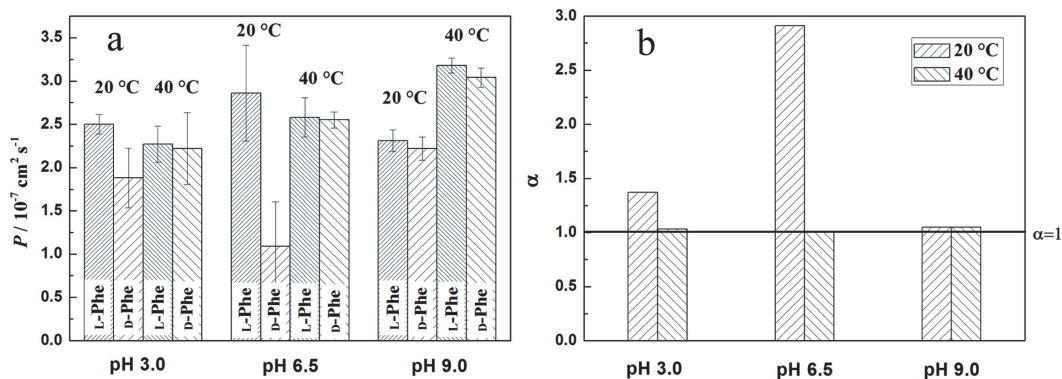


**Fig. 4-4** Permeation coefficients (a) and the permselectivity of L- and D- phenylalanine (b) through the peptide grafted PNIPAm crosslinked membrane.

On the other hand, under the neutral condition, pH 6.5, the peptide graft chains were partially protonated. The electrostatic repulsion among the partially protonated peptide chains disturbed the rapid formation of the disordered aggregation and aided in the formation of  $\beta$ -sheet structure owing to the intermolecular hydrogen bonding. However, the degree of the pH induced conformational transition was very little. This is because of the low graft content of the peptide chain and the high degree of crosslinking of the PNIPAm main chain, which disturbed the formation of regular arrangement of the peptide graft chains.

#### 4-3-3 Permselectivity of L- and D- phenylalanine induced by pH and thermal stimuli

In the previous studies, we have been reported that the  $\beta$ -sheet domain in the

peptide molecular membrane acted as a binding site of the amino acid, which have same chirality with the peptide<sup>23</sup>, and the domain acted as a selective permeation path through the membrane for the amino acid<sup>14</sup>. We investigated the permselectivity of *L*- and *D*-phenylalanine through the peptide grafted PNIPAm network membrane, whose peptide chains consisted of *L*-amino acids. The typical permeation curves of *L*- and *D*-phenylalanine at pH 6.5 and 20 °C were shown in Fig. 4-2. The permeation curves of *L*-phenylalanine had a curvature. The permeability coefficient of *L*-phenylalanine,  $2.86 \times 10^{-7} \text{ cm}^2 \text{ s}^{-1}$ , was very high (self-diffusion constant:  $9.0 \times 10^{-6} \text{ cm}^2 \text{ s}^{-1}$ ). We think that the curvature of the permeation curve due to the cancel of the concentration difference. On the other hand, the permeation of *D*-phenylalanine showed the slight delay time owing to the dissolution of *D*-phenylalanine into the membrane. Fig. 4-4a shows the permeation coefficients of *L*- and *D*-phenylalanine through the membrane under the different pH and temperature conditions. The permeation coefficients were calculated as an averaged value of 3 times measurements. Fig. 4-4b shows the permselectivity,  $\alpha$ , which is the ratio of the permeability coefficient of *L*-phenylalanine to that of *D*-phenylalanine. The permeability of both *L*- and *D*-phenylalanine through the membrane under the basic and high temperature condition (pH 9.0 and 40 °C) were larger than that under the other conditions. Under this condition, the peptide grafted PNIPAm was shrunk in the MF-supported membrane (Table 4-1), and the pore was formed in the membrane. This is the reason for the relatively higher permeability and the non-permselectivity of *L*- and *D*-phenylalanine ( $\alpha=1.0$ , Fig. 4-4b). Under this basic condition at low temperature, 20 °C, the membrane did not show the permselectivity ( $\alpha=1.0$ ). Under this condition, the PNIPAm main chains were hydration, but the peptide graft chain aggregated. The conformation of the membrane disturbed the formation of permselectivity path for the phenylalanine.

Under the acidic condition, pH 3.0, the permeation coefficients of *L*- and *D*-phenylalanine at 20 °C and 40 °C show the same value, and the permselectivity of the phenylalanine did not appeared. Under these conditions, the peptide grafted chains protonated and had the negative charge (pKa of the peptide graft chain was 7.5), and permeant, phenylalanine, was positively charged. This electrostatic repulsion between

the membrane and permeant disturbed the specific interaction in the binding site composed of  $\beta$ -sheet domain in the membrane and resulted in the same permeability of the L- and D- phenylalanine through the membrane above and below the LCST.

On the other hand, under the neutral pH condition, pH 6.5, at 20 °C the significant difference was recognized in the permeability of L- and D- phenylalanine. Under this condition, the membrane was most swollen, and the peptide graft chains were partially protonated and formed considerable amount of  $\beta$ -sheet structure. Furthermore the permeant, phenylalanine, was negatively charged (pI of phenylalanine was 5.48). The attractive force between the negatively charged phenylalanine and the  $\beta$ -sheet peptide domain which was positively charged induced the increasing of the phenylalanine concentration at the interface. The  $\beta$ -sheet peptide domain composed of L-amino acids was acted as effective L-phenylalanine binding site and relatively higher permeability of L-phenylalanine was achieved compared with that of D-isomer ( $\alpha=2.6$ ). Increasing of the temperature, the PNIPAm main chain was dehydration and the polymer was shrunk in the MF-support membrane to form the void. The void acted as the permeable path both the L- and D- phenylalanine, which results in the non-permselectivity through this membrane.

## 4-4 Effect of Crosslinking Degree on the Peptide-grafted Membrane

### 4-4-1 effect of crosslinking degree for conformational changes of the peptide graft chains

Table 4-3 shows pH and thermo-induced hydration degree changes of the crosslinked membranes. The hydration degrees of the low-crosslinked membrane were obviously decreased above the LCST, 36 °C, of the PNIPAm main chain. On the other hand, the thermo-induced hydration

**Table 4-3.** Hydration degrees of crosslinked membranes under various conditions

	Hydration degree / %			
	Low-crosslinked		High-crosslinked	
	20 °C	40 °C	20 °C	40 °C
pH 3.0	98.5	93.8	96.8	96.5
pH 6.5	98.6	86.3	98.2	97.8
pH 9.0	98.9	80.9	96.8	96.3

changes of the high crosslinked membrane were relatively lower than those of the low crosslinked membrane owing to the high crosslinking density.

The conformational changes of the graft peptides of the crosslinked membranes induced by pH and thermo-stimuli were characterized by the TM-FTIR spectra. We obtained the fraction of conformations,  $\alpha$ -helix,  $\beta$ -sheet, and random coil, from the ratio of integrated peak intensities assigned by peak deconvolution of the amide I band<sup>12</sup> (Table 4-4). The graft peptides in the low crosslinked membrane took a mainly  $\alpha$ -helical conformation. On the other hand, in the high crosslinked membrane, the  $\beta$ -sheet contents of the graft peptides were increased. It is well known that the sequential alternating amphiphilic peptide takes a  $\beta$ -sheet conformation. In the low crosslinked membrane, the mobility of the PNIPAm main chain was high owing to the low crosslinking density compared with high crosslinked membrane. The PNIPAm main chain disturbed the intermolecular hydrogen bonding among the graft peptides. This resulted in the low  $\beta$ -sheet contents.

**Table 4-4.** pH and thermo-induced conformational changes of the graft peptide in the membranes

	T	Low-crosslinked			High-crosslinked		
		$\alpha$ -helix / %	$\beta$ -sheet / %	Random / %	$\alpha$ -helix / %	$\beta$ -sheet / %	Random / %
pH 3.0	20 °C	54.8	12.9	32.3	34.9	37.2	27.9
	40 °C	59.6	15.8	24.6	36.4	37.7	25.9
pH 6.5	20 °C	45.2	22.6	32.2	33.3	39.2	27.5
	40 °C	51.6	16.1	32.3	30.7	40.0	29.3
pH 9.0	20 °C	40.0	38.2	21.8	30.3	36.4	33.3
	40 °C	41.4	34.5	24.1	30.6	36.1	33.3

#### 4-4-2 Effect of crosslinking degree on the permeability changes of $L$ - and $D$ -Phe

We investigated the permeability of  $L$ - and  $D$ -Phe through the peptide grafted crosslinked PNIPAm membranes in the support films. Figure 1 shows permeability coefficient of  $L$ - and  $D$ -Phe through the a); low crosslinked membrane, and b); high crosslinked membrane in the support film under the different pH and temperature conditions, respectively. In the case of low crosslinked membrane, the permeability coefficients were very high. The order of the permeability coefficients was  $10^{-6} \text{ cm}^2 \text{ s}^{-1}$  (self-diffusion constant of Phe is  $9.0 \times 10^{-6} \text{ cm}^2 \text{ s}^{-1}$ ). And the low crosslinked

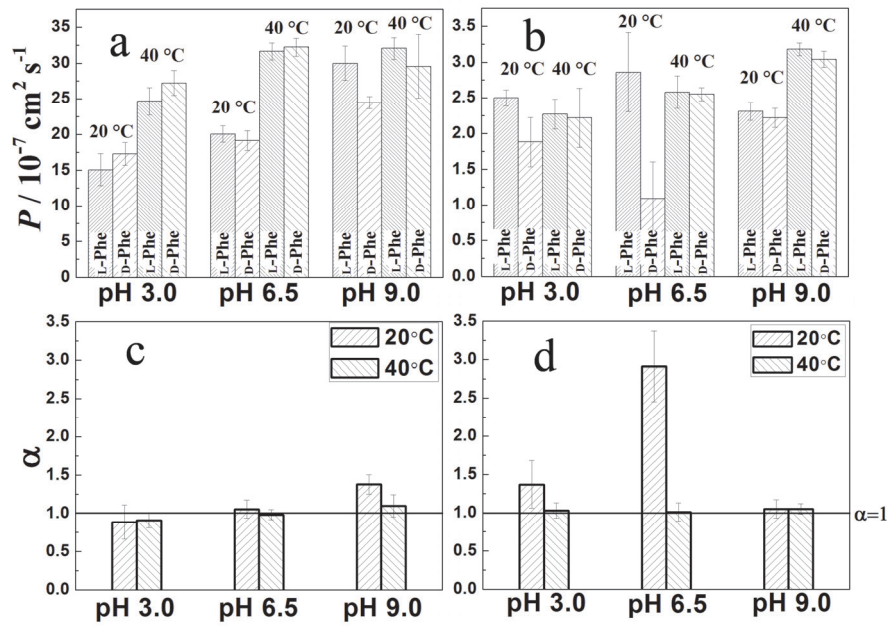


**Fig. 4-5.** Permeability coefficients of  $L$ - and  $D$ -Phe through the a); low crosslinked membrane and b); high crosslinked membrane in the support film, respectively. c) and d) show the permselectivity of  $L$ -Phe to  $D$ -Phe through the low crosslinked membrane and high crosslinked membrane in the support film, respectively.

membrane did not show the permselectivity of  $L$ - and  $D$ -Phe (Fig. 4-5c). The high permeability and low permselectivity of Phe through the low crosslinked membrane was due to flexible structure of the membrane, whose crosslinking degree was low. However, the permeability through the membrane was increased above LCST under the acidic and neutral pH conditions. Above LCST, the PNIPAm main chain was shrunk to form globular conformation. The conformational transition of PNIPAm main chain induced the formation of the pore, which was acted as the permeable path for both  $L$ - and  $D$ -Phe. However, under the basic condition the permeability through the membrane did not change by the thermal stimuli. Under this condition, the deprotonated peptide graft chains formed disordered aggregate owing to the hydrophobic interaction in the membrane. The aggregate acted as physical crosslinker in the membrane and formed permeable path by the disturbance of the homogeneous hydrated membrane structure.

On the other hand, permeability and permselectivity through the high crosslinked membrane showed different phenomenon under the neutral and acidic conditions (Fig. 4-5b and 4-5d). Especially, under the neutral condition (pH 6.5) and low temperature

below LCST (20 °C) the membrane show the relatively high permeability ( $2.86 \times 10^{-7} \text{ cm}^2 \text{ s}^{-1}$ ) and permselectivity ( $\alpha=2.9$ ). Under this condition, the high crosslinked membrane was most swollen and the peptide graft chains were partially protonated (pKa of the peptide graft chain was 7.5). The electrostatic repulsion among the partially protonated peptide chains in the high crosslinked membrane disturbed the rapid formation of the disordered aggregation and aided in the formation of the considerable amount of  $\beta$ -sheet structure, which acted as permselective path for the  $L$ -Phe. Furthermore the permeant, Phe, was negatively charged (PI of Phe was 5.48). The attractive force between the negatively charged Phe and positively charged  $\beta$ -sheet domain induced the increase of the partition of  $L$ -Phe to the membrane. That is to say, the  $\beta$ -sheet domain composed of  $L$ -amino acid in the membrane acted as effective binding site and permeable path for the  $L$ -Phe. With the increasing in temperature above LCST (40 °C), the PNIPAm main chain was dehydrated and the crosslinked membrane was shrunk in the support film to form the void. The void acted as the non-selective permeable path for both  $L$ - and  $D$ -Phe.

Under the acidic condition, the high crosslinked membrane did not show the permselectivity. Under the acidic condition, peptide graft chain and permeant, Phe, had positive charge. The electrostatic repulsion between the membrane and permeant disturbed partition of the Phe to the membrane and resulted in the same permeability of  $L$ - and  $D$ -Phe through the membrane above and below LCST.

## 4-5 Conclusion

In this research we synthesized a peptide grafted PNIPAm network membrane by the UV photopolymerization. This polymer membrane has a chiral selectivity due to the grafted peptide chains. The permeability of the amino acids through this membrane is sensitive to pH and temperature. At the temperature lower than the LCST of PNIPAm and under the neutral pH conditions,  $\beta$ -sheet peptide domain composed of  $L$ -amino acids in the membrane acted as the effective permeable path for its own optically active amino acid ( $L$ -phenylalanine). When temperature is higher



than the LCST of PNIPAm, the shrinking of the PNIPAm main chain formed void structure that acted as permeable paths through the membrane for the both isomer (L- and D- phenylalanine). We think that the permselectivity of the peptide grafted PNIPAm network membrane could be improve for the practical application by the decreasing of crosslinking and increasing of peptide graft chains.

## Reference

1. Norbert M. Maier, Pilar Franco & Wolfgang Lindner, Separation of enantiomers: needs, challenges, perspectives, *Journal of Chromatography A*. **906**, 3-33 (2001).
2. Carlos A. M. Afonso & João G. Crespo, Recent Advances in Chiral Resolution through Membrane-Based Approaches, *Angewandte Chemie International Edition*. **43**, 5293-5295 (2004).
3. Kshama B. Jirage & Charles R. Martin, New developments in membrane-based separations, *Trends in biotechnology*. **17**, 197-200 (1999).
4. Hava Caner, Efrat Groner, Liron Levy & Israel Agranat, Trends in the development of chiral drugs, *Drug Discovery Today*. **9**, 105-110 (2004).
5. Michael Breuer, Klaus Ditrich, Tilo Habicher, Bernhard Hauer, Maria Keßeler, Rainer Stürmer & Thomas Zelinski, Industrial Methods for the Production of Optically Active Intermediates, *Angewandte Chemie International Edition*. **43**, 788-824 (2004).
6. Sonia Keunchkarian, Carlos A. Franca, Leonardo G. Gagliardi & Cecilia B. Castells, Enantioseparation of  $\alpha$ -amino acids by means of Cinchona alkaloids as selectors in chiral ligand-exchange chromatography, *Journal of Chromatography A*. **1298**, 103-108 (2013).
7. S. Robl, L. Gou, A. Gere, M. Sordo, H. Lorenz, A. Mayer, C. Pauls, K. Leonhard, A. Bardow, A. Seidel-Morgenstern & K. Schaber, Chiral separation by combining pertraction and preferential crystallization, *Chemical Engineering and Processing: Process Intensification*. **67**, 80-88 (2013).
8. Edwin Vedejs & Mara Jure, Efficiency in Nonenzymatic Kinetic Resolution, *Angewandte Chemie International Edition*. **44**, 3974-4001 (2005).

9. R. Xie, L. Y. Chu & J. G. Deng, Membranes and membrane processes for chiral resolution, *Chemical Society reviews*. **37**, 1243-1263 (2008).
10. Toshiki Aoki, Masayuki Kokai, Ken-ichi Shinohara & Eizo Oikawa, Chiral Helical Conformation of the Polyphenylacetylene Having Optically-Active Bulky Substituent, *Chemistry Letters*. **22**, 2009-2012 (1993).
11. Toshiki Aoki, Syouji Tomizawa & Eizo Oikawa, Enantioselective permeation through poly[ $\gamma$ -[3-(pentamethyldisiloxanyl)propyl]-L-glutamate] membranes, *Journal of Membrane Science*. **99**, 117-125 (1995).
12. Teruyuki Masawaki, Satoshi Matsumoto & Setsuji Tone, Enantioselective Permeation of Amino Acid Isomers through L-Phenylglycine-Fixed Membranes at Pressure Gradient, *JOURNAL OF CHEMICAL ENGINEERING OF JAPAN*. **27**, 517-522 (1994).
13. Atsushi Maruyama, Noriyuki Adachi, Takehisa Takatsuki, Masanori Torii, Kohei Sanui & Naoya Ogata, Enantioselective permeation of  $\alpha$ -amino acid isomers through poly(amino acid)-derived membranes, *Macromolecules*. **23**, 2748-2752 (1990).
14. M. Higuchi & T. Kinoshita, Specific permeability of chiral amino acids through functional molecular membranes composed of an amphiphilic graft peptide, *Chemphyschem : a European journal of chemical physics and physical chemistry*. **9**, 1110-1113 (2008).
15. Yusuf Yagci, Steffen Jockusch & Nicholas J. Turro, Photoinitiated Polymerization: Advances, Challenges, and Opportunities, *Macromolecules*. **43**, 6245-6260 (2010).
16. John F. Quinn, Leonie Barner, Christopher Barner-Kowollik, Ezio Rizzardo & Thomas P. Davis, Reversible Addition-Fragmentation Chain Transfer Polymerization Initiated with Ultraviolet Radiation, *Macromolecules*. **35**, 7620-7627 (2002).
17. Mehmet Atilla Tasdelen, Yasemin Yuksel Durmaz, Bunyamin Karagoz, Niyazi Bicak & Yusuf Yagci, A new photoiniferter/RAFT agent for ambient temperature rapid and well-controlled radical polymerization, *Journal of Polymer Science Part A: Polymer Chemistry*. **46**, 3387-3395 (2008).
18. Meng Yu, Tang Tang, Akinori Takasu & Masahiro Higuchi, pH- and thermo-induced morphological changes of an amphiphilic peptide-grafted copolymer in solution, *Polymer Journal*.
19. Etsuko Yoshinari, Hidemitsu Furukawa & Kazuyuki Horie, Fluorescence study on the

mechanism of rapid shrinking of grafted poly(N-isopropylacrylamide) gels and semi-IPN gels, *Polymer*. **46**, 7741-7748 (2005).

20. Liang Liang, Xiangdong Feng, Loni Peurrung & Vish Viswanathan, Temperature-sensitive membranes prepared by UV photopolymerization of N-isopropylacrylamide on a surface of porous hydrophilic polypropylene membranes, *Journal of Membrane Science*. **162**, 235-246 (1999).

21. Hiroshi Inomata, Shuichi Goto, Katsuto Otake & Shozaburo Saito, Effect of additives on phase transition of N-isopropylacrylamide gels, *Langmuir*. **8**, 687-690 (1992).

22. G. Bokias, G. Staikos & I. Iliopoulos, Solution properties and phase behaviour of copolymers of acrylic acid with N-isopropylacrylamide: the importance of the intrachain hydrogen bonding, *Polymer*. **41**, 7399-7405 (2000).

23. Masahiro Higuchi, Jonathan P. Wright, Kazuhiro Taguchi & Takatoshi Kinoshita, Structure and Molecular Recognition Properties of a Poly(allylamine) Monolayer Containing Poly(L-alanine) Graft Chains, *Langmuir*. **16**, 7061-7065 (2000).

# Chapter 5

## Controlled Release of Enantiomers in Peptide Grafted PNIPAm Gels

### 5-1 Introduction

Swollen polymer networks, also called polymer gels received attention in biology and medicine as functional matrices to exogenously stimulate cells for both in vitro and in vivo applications<sup>1</sup>. A gel is generally considered to be a three-dimensional polymer network swollen by a large amount of solvent. In one way, polymer gels can be generally classified into so-called “chemical” and “physical” gels. A chemical gel is normally formed via the copolymerization of monomers with a cross-linking agent, in which polymer chains are interconnected by covalent bonds. Poly(*N*-isopropylacrylamide) (PNIPAm) has aroused great interest for many years<sup>2</sup> because of its interesting thermal properties; in water, it is characterized by a sharp volume phase transition at a lower critical solution temperature (LCST)<sup>3</sup>. By copolymerizing with a divinyl group of cross-linker, *N,N*-methylenebis(acrylamide) (BisAAM), this polymer can form a hydrogel, a water-containing polymer chain network. Tanaka’s early work on bulk *N*-isopropylacrylamide (NIPAm) hydrogels using simple microscopic observation and subsequent studies has led to a good understanding of the gel phase transition properties<sup>4-6</sup>. By exploiting the unique thermal properties of NIPAm gels, materials for many interesting applications including controlled drug delivery<sup>7</sup>, artificial muscles<sup>8</sup>, shape memory<sup>9</sup>, sensors<sup>10</sup>, and chromatography<sup>11</sup> have been designed.

Controlled drug delivery technology represents one of the most rapidly advancing areas of science in which chemists and chemical engineers are contributing to human health care<sup>12</sup>. Such delivery systems offer numerous advantages compared to conventional dosage forms including improved efficacy, reduced toxicity, and improved patient compliance and convenience. Such systems often use synthetic

polymers as carriers for the drugs. By so doing, treatments that would not otherwise be possible are now in conventional use. Among many drug delivery systems, polymeric controlled-release drug delivery systems have attracted great attention of many polymer scientists in recent years due to their potential applications. And smart hydrogels were extensively investigated as intelligent carries among the polymeric controlled-release drug delivery system<sup>13,14</sup>. This is due to the fact that the diffusion and permeation of drug molecules (or solutes) from the hydrogels can be controlled by external stimuli. Among smart polymers, poly(*N*-isopropylacrylamide) (PNIPAm) was widely investigated as drug (or solute) carriers, owing to PNIPAm's thermosensitivity and leading to a temperature-modulated drug release. As we introduced in former chapters, PNIPAm undergoes a volume phase transition at a critical temperature ( $T_C$ ) of 34 °C. Below  $T_C$ , it is hydrophilic and swells in water, while above  $T_C$ , it becomes hydrophobic and expels water, collapsing into a smaller volume. The crosslinked PNIPAm gel is a widely studied thermosensitive gel that exhibits discontinuous phase separation when the external temperature is increased.

Polymer based drug or vaccine delivery systems have attracted much attention due to their ability to perform multiple critical functions. Degradable polymer is the most widely studied delivery system, but the byproducts obtained in the degradation of a polymer carrier are an important problem of this system. Our work is aimed to develop an environmental sensitive with chiral separation drug delivery vehicle. The dual-responsive peptide grafted PNIPAm that we synthesized before give a possibility for this purpose. In this part we synthesized the peptide grafted PNIPAm gels, and using phenylalanine as guest biomolecule to investigate the stimuli responsive release of the gel.

## **5-2 Experimental Section**

### **5-2-1 Preparation of peptide grafted PNIPAm gels**

The peptide grafted PNIPAm gel was prepared by UV irradiated polymerization.

The peptide, (Leu-Lys)<sub>8</sub>-vinyl (52 mg), was solved in 1 ml deionized water with nipam (25 mg). After the monomers were dissolved, the crosslinker *N,N'*-methylenebisacrylamide (BisAAM, Nacalai tesque, Kyoto, Japan) (2 mg) and initiator 2-Hydroxy-4'-(2-hydroxyethoxy)-2-methylpropiophenone (photocure 2959, Aldrich, USA) (1 mg) were added into the monomer solution. To remove the oxygen from the reaction mixture, three freeze-pump-thaw cycles were performed. Then the reaction solution was irradiated under the UV light (HLR 100T-2, SEN LIGHTS Corporation, Japan) for 30 minutes. After polymerization the gel products were immersed in deionized water for 2 days to remove the unreacted monomers. Then the gels were lyophilized to obtain the final products for further characterization. The composition of peptide grafted PNIPAm gel was characterized by the elemental analysis (Vario EL cube, Elementar Corporation, Germany). From the element analysis we calculated the molar ratio of NIPAM; 0.91, peptide graft chain; 0.01, cross linker; 0.08, respectively. The peptide content is much lower, because of the three-dimensional network structure blocked the introduction of peptide grafted chains into the PNIPAm main chains.

### **5-2-2 Swelling study of PNIPAm gels**

Here we use the water content of swollen membrane indicated the degree of hydration of the PNIPAm gel. The dried gels were immersed in aqueous solution under various conditions for two days to reach the equilibrium state. For each condition, the excess water on the swollen hydrogel surface was removed with filter paper and the weight of the swollen sample was determined, then the swollen sample was put into the vacuum drier to get the dried gel and weighted. The swollen ratios were calculated by the equation:  $S = (M_s - M_0) / M_s$ , where  $M_s$  is the weight of swollen gel and  $M_0$  is the weight of dried gel.

### **5-2-3 FT-IR measurements**

Secondary structural changes of the peptide graft chains in the PNIPAm gel under different pH were estimated by Transmittance Fourier transform infrared (TM-FTIR)

spectroscopy. The TM-FTIR spectra were measured with a Perkin-Elmer Spectra 2000 (reduction: 4 cm<sup>-1</sup>, number of scan: 32). The gels were dipped in aqueous solutions at different pH and quickly frozen in liquid nitrogen, and then the frozen samples were lyophilized to obtain the dried gel samples. The pellets for TM-FTIR measurements were prepared by the mixing of the membrane powder and KBr. The weight fraction of the membrane was fixed at 1 wt%.

#### **5-2-4 Release study of the gels**

The dried gels were immersed in 0.1 M L-Phe and D-Phe aqueous solution at 20 °C respectively for three days reached to a constant weight. Then the swollen gels were dropped into 10 mL deionized water, the concentration of solute ( $C_s$ ) that peptide grafted PNIPAm gel released was measured using a calibration curve at the wavelength 256.5 nm where the phenylalanine shows the maximum absorbance, quantitatively determined by UV-vis spectrophotometer (UV-3600, Shimadzu, Japan). The release property of this gel was indicated by the release amount of unit weight Phe ( $M_r$ ),

$$M_r = (C_s \times 10) / M_0$$

where  $M_0$  is the weight of dried gel.

### **5-3 Results and discussion**

#### **5-3-1 degree of hydration of the swollen peptide grafted PNIPAm gels**

By copolymerizing with the divinyl group cross-linker BisAAM, this polymer can form a hydrogel, a water-containing polymer chain network. In this research we use the water content of swollen gel indicated the degree of hydration of the PNIPAm gel. Table 5-1 listed the hydration of the gel under various conditions. The hydration degree reached the maximum value 98.3% at 20 °C and pH 6.5, that under

**Table 5-1** The degree of hydration of the peptide grafted PNIPAm gel under different conditions

pH	20 °C			40 °C		
	3.0	6.5	9.0	3.0	6.5	9.0
<b>S</b>	94.5%	98.3%	93.2%	86.4%	91.2%	88.8%

this condition the PNIPAm was hydrophilic and formed expand structure. As temperature increased to 40 °C, which is higher than the LCST temperature of PNIPAm, the PNIPAm formed compact structures by dehydration<sup>15</sup>. However the grafted peptide chains played as a volume exclusion part disturbed the shrinkage of PNIPAm gel, as a result the degree of hydration has decreased but slighter than common PNIPAm gels.

### **5-3-2 pH-induced conformational transition of the peptides graft chain in the PNIPAm gel**

We investigated the conformational changes of the peptide graft chains in the gel at 20 °C by the TM-FTIR measurements. The samples for TM-FTIR measurements were prepared as follows, the polymer gel was dipped in the aqueous solutions, which was adjusted to designed pH. The solutions contained gels were quickly frozen in liquid nitrogen and lyophilized to obtain measurement samples. Fig. 5-1 shows the TM-FTIR absorption spectra of the polymer gels under different pH. In the spectra, characteristic absorptions of the amide I band with  $\alpha$ -helix,  $\beta$ -sheet, and random coil conformations were observed at 1650, 1630, and 1675  $\text{cm}^{-1}$ , respectively<sup>16</sup>. The ratio of integrated peak intensities assigned to individual secondary structure, which was obtained by peak deconvolution of the amide I band,



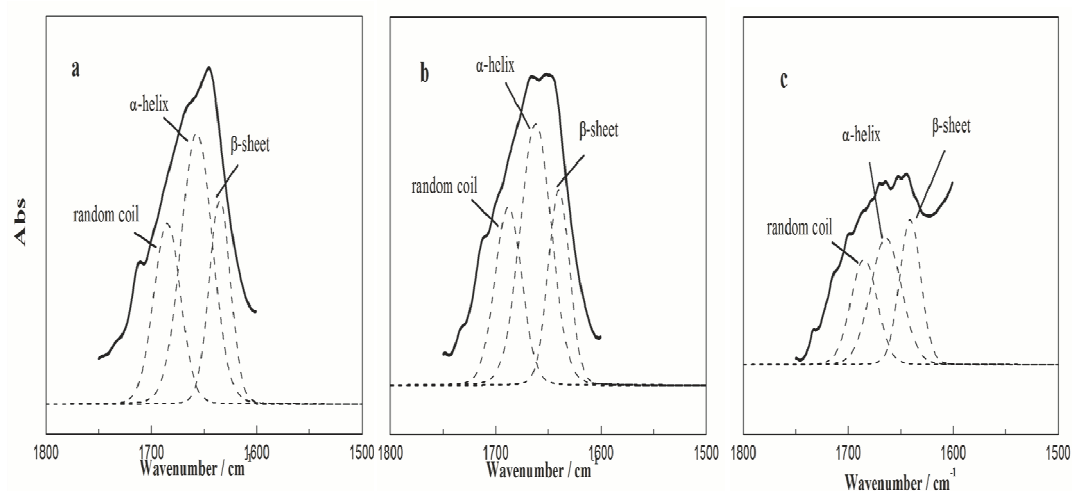


**Fig. 5-1.** TM-FTIR spectra of peptide graft chains in the PNIPAm gel at a) pH 3.0; b) pH 6.5; c) pH 9.0 respectively. Broken lines show the peak deconvolution of the amide I band.

gave the percentage of conformational changes of the peptide graft chain in the gels. The results of conformational analysis were summarized in Table 5-2. From the result we can find that the conformation changes of peptide graft chain in the PNIPAm gel show the same tendency as the membrane system.  $\alpha$ -helix was the main structure of PNIPAm gel but  $\beta$ -sheet structure was increased with pH condition changed from acidic to basic. However, because of the low grafting ratio, the content of  $\beta$ -sheet structure in gel system was lower than the membrane system.

**Table. 5-2** pH- induced conformation changes of the peptide graft chain in the PNIPAm gel.

	Conformation		
	$\alpha$ -helix / %	$\beta$ -sheet / %	Random coil / %
pH 3.0	48.0	24.6	27.4
pH 6.5	47.7	24.4	27.9
pH 9.0	40.0	31.4	28.6

### 5-3-3 Stimuli-induced controlled release of L- and D- phenylalanine

As we investigated before, the peptide grafted PNIPAm gel showed most swollen structure in neutral condition (pH 6.5) at 20 °C. So in this research we let the PNIPAm gels to absorb the 0.1 M L- or D- phenylalanine solution under this condition (pH 6.5, 20 °C) reach to the equilibrium state. Then the swollen gel was dropped into 10 mL

deionized water to release the phenylalanine, concentration of the phenylalanine was calculated by UV absorbance at 256.5 nm according to a calibration curve. Fig. 5-2 shows the release of  $L$ -phenylalanine released from unit weight gel depends on time at different pH. It is apparent that a rapid release of Phe was showed within the first 30 minutes, which was most likely due to those amino acids which were incorporated in the gel rapidly escaped into the supernatant solution. In this figure, the early release rate of  $L$ -Phe at the initial stage under the basic condition (pH 9.0) was decline. Under this condition, the  $\beta$ -sheet content of grafted peptides in the gel was slightly higher than that under acidic and neutral conditions. According to our previous study<sup>17,18</sup>, the  $\beta$ -sheet domain acted as a specific binding site for its own optical active amino acid. In the diffusion process of guest from gel inside to outside solution, the guest was absorbed in the  $\beta$ -sheet domain. The  $\beta$ -sheet domain acted similar to the molecular sieve for  $L$ -Phe. This means the increasing of  $\beta$ -sheet content in the gel

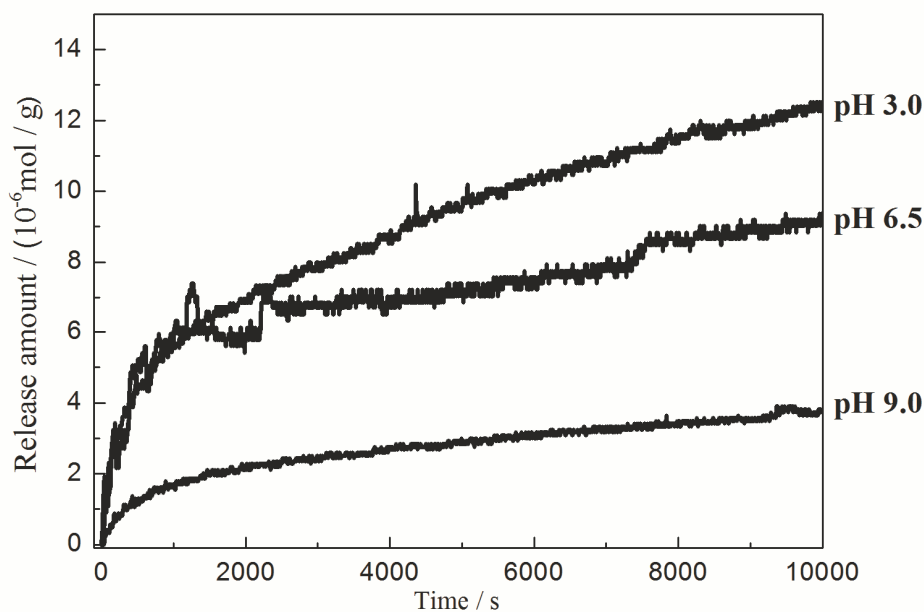


**Fig. 5-2.** Release amount of  $L$ -phenylalanine depend on time at various pH conditions at 20°C.

decreased the release of  $L$ -Phe. The initial release of  $L$ -Phe and  $D$ -Phe at 20 °C and pH 6.5 are shown in the Fig. 5-3. The release of  $D$ -Phe was faster than that of  $L$ -Phe because the  $\beta$ -sheet domain acted as binding site of the  $L$ -Phe and this absorption effect disturbed the release of the  $L$ -Phe.

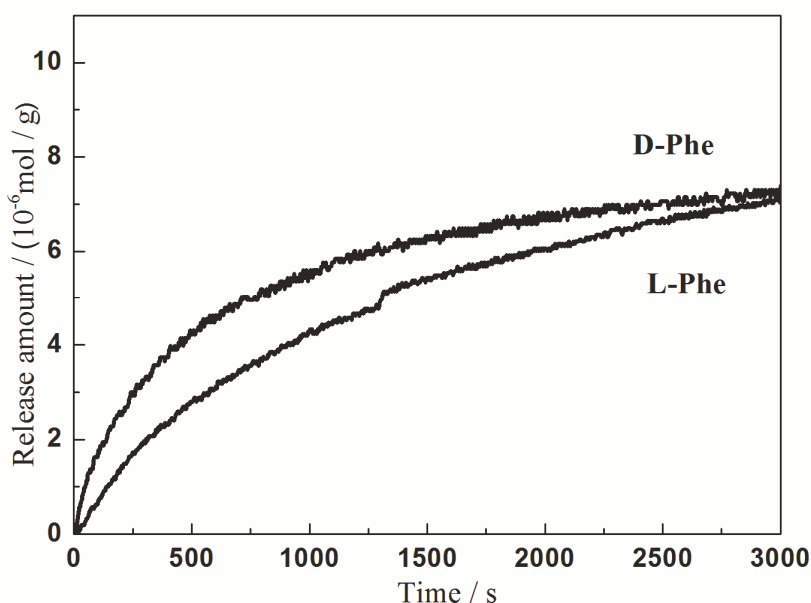


**Fig. 5-3.** Release amount of <sub>L</sub>- and <sub>D</sub>- phenylalanine depend on time at 20 °C and pH 6.5.

As temperature increased to 40 °C, which is higher than the LCST of PNIPAm, the release of both <sub>L</sub>- and <sub>D</sub>- Phe had a obviously increase compared with that at 20 °C. Fig. 5-4 shows the comparison of release of phenylalanine at different temperature under the neutral condition (pH 6.5). This is because of the hydrophobic transition of PNIPAm network above the LCST, this transition led to the volume shrinkage of the PNIPAm gel. The shrinkage of the PNIPAm gel excluded the Phe that make the release process faster. It is also known that the volume phase transition of the PNIPAm polymeric gel is accompanied by the dehydration of NIPAM chains<sup>19</sup>. The dehydrated polymeric chains (Table. 5-1) determine the hydrophobic behavior of the collapsed gel. A decrease in the water content, thus a decrease in the polarity of the system, and an increase in the hydrophobic of the polymeric chains above the volume phase transition temperature must result in a more effective removal of deprotonated phenylalanine from the gel system<sup>20</sup>. This effect may explain the larger values of release parameters for the Phe.

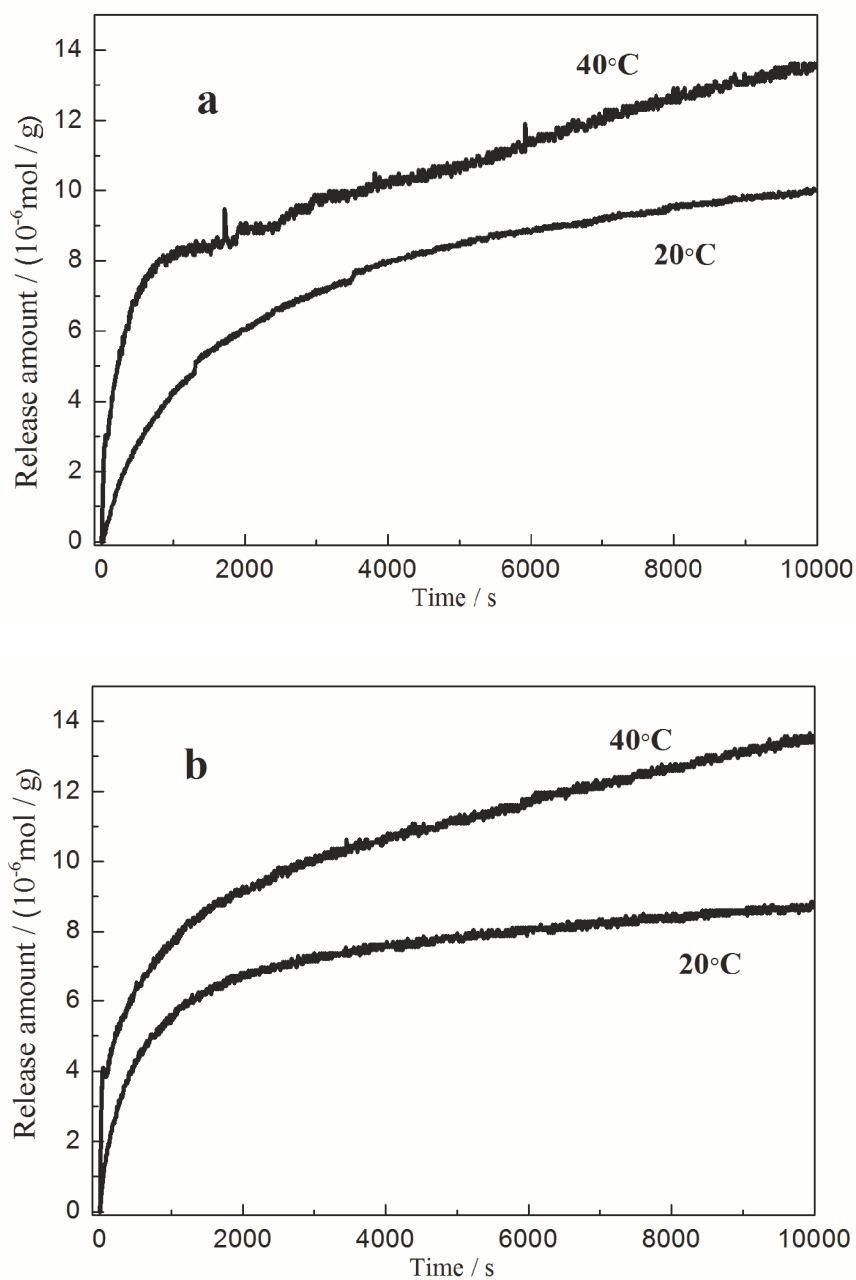


**Fig. 5-4.** Thermal-induced release amount changes of (a) L-Phe and (b) D-Phe depend on time at pH 6.5.

## 5-4 Conclusion

In this chapter, an attempt was made to synthesize a kind of controlled released gel which could response to temperature and pH changes. The peptide (LK)<sub>8</sub> grafted PNIPAm hydrogel could be prepared by the irradiation initiated radical polymerization. The composition of the gel was confirmed by element analysis, and the conformational changes induced by pH condition were investigated by the

TM-FTIR spectrum. We developed this peptide grafted PNIPAm gel to be a drug delivery vehicle; L-Phe and D-Phe were used as model guests to characterize the controlled release property which was induced by temperature. Because of the same optical activity, the  $\beta$ -sheet domain acted as binding site of L-Phe decreased the release of L-Phe. And as temperature increased higher than LCST, the hydrophobic transition of PNIPAm led to the shrinkage of PNIPAm gel. As a result the release of both L-Phe and D-Phe were increased compared with 20 °C. For the future application, we think this peptide graft PNIPAm gel could be used not only in drug delivery system but also in the agriculture field such as fertilizer retention and desertification control.

## Reference

1. Jens-Uwe Sommer, Ron Dockhorn, Petra B. Welzel, Uwe Freudenberg & Carsten Werner, Swelling Equilibrium of a Binary Polymer Gel, *Macromolecules*. **44**, 981-986 (2011).
2. HG Schild, Poly (N-isopropylacrylamide): experiment, theory and application, *Progress in polymer science*. **17**, 163-249 (1992).
3. Chi Wu, A comparison between the 'coil-to-globule' transition of linear chains and the "volume phase transition" of spherical microgels, *Polymer*. **39**, 10 (1998).
4. Yoshiharu Hirose, Takayuki Amiya, Yoshitsugu Hirokawa & Toyochi Tanaka, Phase transition of submicron gel beads, *Macromolecules*. **20**, 1342-1344 (1987).
5. Eriko Sato Matsuo & Toyochi Tanaka, Kinetics of discontinuous volume-phase transition of gels, *The Journal of Chemical Physics*. **89**, 1695-1703 (1988).
6. Yong Li & Toyochi Tanaka, Kinetics of swelling and shrinking of gels, *The Journal of Chemical Physics*. **92**, 1365-1371 (1990).
7. Allan S Hoffman, Applications of thermally reversible polymers and hydrogels in therapeutics and diagnostics, *Journal of Controlled Release*. **6**, 297-305 (1987).
8. Yoshihito Osada & Simon B Ross-Murphy, Intelligent gels, *Scientific American*. **268**,

82-87 (1993).

9. Zhibing Hu, Xiaomin Zhang & Yong Li, Synthesis and application of modulated polymer gels, *Science*. **269**, 525-527 (1995).
10. John H Holtz & Sanford A Asher, Polymerized colloidal crystal hydrogel films as intelligent chemical sensing materials, *Nature*. **389**, 829-832 (1997).
11. Akihiko Kikuchi & Teruo Okano, Intelligent thermoresponsive polymeric stationary phases for aqueous chromatography of biological compounds, *Progress in polymer science*. **27**, 1165-1193 (2002).
12. Kathryn E Uhrich, Scott M Cannizzaro, Robert S Langer & Kevin M Shakesheff, Polymeric systems for controlled drug release, *Chemical reviews*. **99**, 3181-3198 (1999).
13. Allan S. Hoffman, Hydrogels for biomedical applications, *Advanced Drug Delivery Reviews*. **54**, 3-12 (2002).
14. Annette Rösler, Guido W. M. Vandermeulen & Harm-Anton Klok, Advanced drug delivery devices via self-assembly of amphiphilic block copolymers, *Advanced Drug Delivery Reviews*. **53**, 95-108 (2001).
15. Liang Liang, Xiangdong Feng, Loni Peurrung & Vish Viswanathan, Temperature-sensitive membranes prepared by UV photopolymerization of N-isopropylacrylamide on a surface of porous hydrophilic polypropylene membranes, *Journal of Membrane Science*. **162**, 235-246 (1999).
16. Teruyuki Masawaki, Satoshi Matsumoto & Setsuji Tone, Enantioselective Permeation of Amino Acid Isomers through L-Phenylglycine-Fixed Membranes at Pressure Gradient, *JOURNAL OF CHEMICAL ENGINEERING OF JAPAN*. **27**, 517-522 (1994).
17. Masahiro Higuchi, Jonathan P. Wright, Kazuhiro Taguchi & Takatoshi Kinoshita, Structure and Molecular Recognition Properties of a Poly(allylamine) Monolayer Containing Poly(l-alanine) Graft Chains, *Langmuir*. **16**, 7061-7065 (2000).
18. M. Higuchi & T. Kinoshita, Specific permeability of chiral amino acids through functional molecular membranes composed of an amphiphilic graft peptide, *Chemphyschem : a European journal of chemical physics and physical chemistry*. **9**, 1110-1113 (2008).
19. Katsuto Otake, Hiroshi Inomata, Mikio Konno & Shozaburo Saito, Thermal analysis of the volume phase transition with N-isopropylacrylamide gels, *Macromolecules*. **23**, 283-289

(1990).

20. Wojciech Hyk, Marcin Karbarz, Zbigniew Stojek & Malgorzata Ciszowska, Efficiency of Solute Release from Thermoresponsive Poly(N-isopropylacrylamide) Gels: Electrochemical Studies, *The Journal of Physical Chemistry B*. **108**, 864-868 (2003).

## Chapter 6 Conclusion

A variety of amphiphilic peptides were synthesized, which could form regular secondary structures. The conformational changes of these peptides were examined to investigate the responsibility to the environmental pH changes. Among these amphiphilic peptides, (Leu-Lys)<sub>8</sub>-vinyl is sensitive to the pH. The (Leu-Lys)<sub>8</sub>-vinyl reversibly transferred from random coil conformation structure to regular  $\beta$ -sheet structure by the pH changes acidic to basic condition. The vinyl group of this peptide gives a promising future that introduce into other stimuli-sensitive polymer to prepare the multi-responsive polymers.

In chapter 3 the amphiphilic copolymer, (Leu-Lys)<sub>8</sub>-grafted poly(*N*-isopropylacrylamide), shows pH- and thermo-induced conformational and morphological transitions in aqueous solution. Under acidic conditions, the peptide graft chains were protonated and positively charged, and LKNIPAm formed nanoparticles owing to the electrostatic repulsion among the graft chains above and below the coil-to-globule transition temperature of the PNIPAm main chain. However, under basic conditions, the peptide graft chains were neutral, and at a low temperature below the transition temperature of the main chain, LKNIPAm formed a micellar structure. Only at a high temperature above the transition temperature, in which the main chain formed shrunken globules, did the peptide graft chains form a stable  $\beta$ -sheet structure. The  $\beta$ -sheets of the grafted chains acted as bridging points between the LKNIPAm globules, resulting in the formation of a large aggregated body. We believe that these studies of the structural regulation of multi-stimuli responsive polymers provide useful information for the development of novel stimuli-responsive materials with a wide range of applications in nanotechnology. Because of environmental friendly and high initiation efficiency, we chose photopolymerization to synthesis the polymers for the investigation of further applications.

Chapter 4 gives the application of this dual-responsive copolymer. In this chapter we synthesized a peptide grafted PNIPAm network membrane by the UV



photopolymerization. This polymer membrane has a chiral selective permeability due to the grafted peptide chains. The permeability of the amino acids through this membrane is sensitive to pH and temperature. At the temperature lower than the LCST of PNIPAm and under the neutral pH conditions,  $\beta$ -sheet peptide domain composed of L-amino acids in the membrane acted as the effective permeable path for its own optically active amino acid (L-phenylalanine). When temperature is higher than the LCST of PNIPAm, the shrinkage of the PNIPAm main chain formed void structure that acted as permeable paths through the membrane for the both isomer (L- and D- phenylalanine). We think that the permselectivity of the peptide grafted PNIPAm network membrane could be improve for the practical application by the decreasing of crosslinking and increasing of peptide graft chains.

In chapter 5, an attempt was made to synthesize a kind of controlled released gel which could response to temperature and pH changes. The peptide (LK)<sub>8</sub> grafted PNIPAm hydrogel could be prepared by the irradiation initiated radical polymerization. The composition of the gel was confirmed by element analysis, and the conformational changes induced by pH condition were investigated by the TM-FTIR spectrum. We developed this peptide grafted PNIPAm gel to be a drug delivery vehicle; L-Phe and D-Phe were used as model guests to characterize the controlled release property which was induced by external stimuli. The release of L-Phe decreased with the increasing of pH, because of the interaction between  $\beta$ -sheet structure and L-Phe. When the temperature was higher than LCST, the release of both L- and D- Phe were increased for the shrinkage of PNIPAm gel. For the future application, we think this peptide graft PNIPAm gel could be used not only in drug delivery system but also in the agriculture field such as fertilizer retention and desertification control.

In this research, we focused on the preparation of 16-residues peptide grafted poly(*N*-isopropylacrylamide) which is sensitive to both pH and thermal conditions. And we also investigated the application of this polymer in the field of chiral separation and drug delivery. Because the various kinds of the 16 residues which formed the peptide, we could synthesized many kinds of this peptide grafted PNIPAm

with different properties by this method. We believe this kind of polymer promised a widely application in the field of industrial production and daily life.

## Publications

1. Meng, Yu, Tang Tang, Akinori Takasu and Masahiro, Higuchi. pH- and thermo-induced morphological changes of an amphiphilic peptide-grafted copolymer in solution. *Polym. J.* 2014, **46**, 52–58.
2. Meng, Yu, Kenji, Nagata and Masahiro Higuchi. pH- and Thermo-induced Specific Permeability of Chiral Amino Acids through the Peptide Grafted Poly(N-isopropylamide) Network Membrane. *Journal of the Society of Fiber Science and Technology, Japan.* 2013, **69**, 245-250.
3. Meng, Yu and Masahiro Higuchi. Specific Permeability of Chiral Amino Acids through the Peptide Grafted Poly (N-isopropylacrylamide) Crosslinked Membranes. *Trans. MRS-J.* 2014. *In press.*

## Conference

1. Meng, Yu, Akinori Takasu and Masahiro, Higuchi. pH and Thermo-induced Morphological Changes of the Amphiphilic Peptide Grafted Copolymer Assembly in Solution. **Poster.** 62<sup>th</sup> SPSJ Symposium on Macromolecules, 2013, Kyoto, Japan.
2. Meng, Yu and Masahiro, Higuchi. Specific Permeability of Chiral Amino Acids through the Peptide Grafted Poly (N-isopropylacrylamide) Crosslinked Membranes. **Poster.** 23<sup>rd</sup> annual meeting of MRS-Japan 2013, Yokohama, Japan.